

# Role of CFTR in diabetes-induced pancreatic ductal fluid and $\text{HCO}_3^-$ secretion

Attila Ébert<sup>1,2</sup> , Eleonóra Gál<sup>1</sup>, Emese Tóth<sup>3,4</sup>, Titanilla Szögi<sup>5</sup>, Péter Hegyi<sup>3,6,7,8</sup>   
and Viktória Venglovecz<sup>1,6</sup> 

<sup>1</sup>Department of Pharmacology and Pharmacotherapy, University of Szeged, Szeged, Hungary

<sup>2</sup>ELI ALPS, ELI-HU Non-Profit Ltd, Szeged, Hungary

<sup>3</sup>Translational Pancreatology Research Group, Interdisciplinary Center of Excellence for Research Development and Innovation, University of Szeged, Szeged, Hungary

<sup>4</sup>Department of Health Sciences, Department of Theoretical and Integrative Health Sciences, University of Debrecen, Debrecen, Hungary

<sup>5</sup>Department of Pathology, University of Szeged, Szeged, Hungary

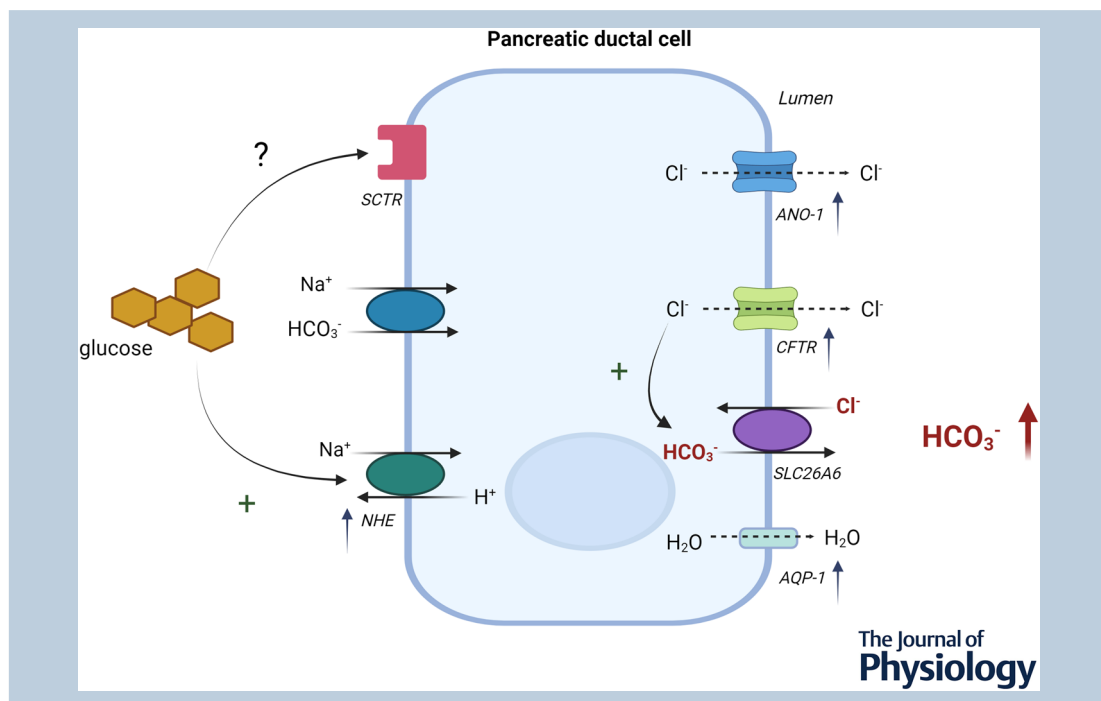
<sup>6</sup>Institute for Translational Medicine, Szentágotthai Research Centre, Medical School, University of Pécs, Pécs, Hungary

<sup>7</sup>Centre for Translational Medicine, Semmelweis University, Budapest, Hungary

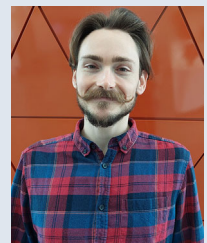
<sup>8</sup>Division of Pancreatic Diseases, Heart and Vascular Center, Semmelweis University, Budapest, Hungary

Handling Editors: Kim Barrett & Pawel Ferdek

The peer review history is available in the Supporting Information section of this article (<https://doi.org/10.1113/JP285702#support-information-section>).



**Attila Ébert** is a PhD candidate at the Department of Pharmacology and Pharmacotherapy, University of Szeged, supervised by Dr Viktória Venglovecz. Attila obtained his MSc degree in molecular biology, microbiology and immunology at the Faculty of Science and Informatics, University of Szeged. His current research focuses on exocrine and endocrine pancreas interactions and pancreatogenic diabetes. His goal is to identify the physiological processes that lead to pancreatic disease and identify new targets for development of therapy. He is also currently working on the field of radiation biology and will continue to do pancreas research with a multidisciplinary approach.



**Abstract** Type 1 diabetes is a disease of the endocrine pancreas; however, it also affects exocrine function. Although most studies have examined the effects of diabetes on acinar cells, much less is known regarding ductal cells, despite their important protective function in the pancreas. Therefore, we investigated the effect of diabetes on ductal function. Diabetes was induced in wild-type and cystic fibrosis transmembrane conductance regulator (CFTR) knockout mice following an i.p. administration of streptozotocin. Pancreatic ductal fluid and  $\text{HCO}_3^-$  secretion were determined using fluid secretion measurements and fluorescence microscopy, respectively. The expression of ion transporters was measured by real-time PCR and immunohistochemistry. Transmission electron microscopy was used for the morphological characterization of the pancreas. Serum secretin and cholecystokinin levels were measured by an enzyme-linked immunosorbent assay. Ductal fluid and  $\text{HCO}_3^-$  secretion, CFTR activity, and the expression of CFTR,  $\text{Na}^+/\text{H}^+$  exchanger-1, anoctamine-1 and aquaporin-1 were significantly elevated in diabetic mice. Acute or chronic glucose treatment did not affect  $\text{HCO}_3^-$  secretion, but increased alkalizing transporter activity. Inhibition of CFTR significantly reduced  $\text{HCO}_3^-$  secretion in both normal and diabetic mice. Serum levels of secretin and cholecystokinin were unchanged, but the expression of secretin receptors significantly increased in diabetic mice. Diabetes increases fluid and  $\text{HCO}_3^-$  secretion in pancreatic ductal cells, which is associated with the increased function of ion and water transporters, particularly CFTR.

(Received 20 September 2023; accepted after revision 17 January 2024; first published online 22 February 2024)

**Corresponding author** V. Venglovecz: Department of Pharmacology and Pharmacotherapy, University of Szeged, H-6720 Szeged, Hungary. Email: venglovecz.viktoria@med.u-szeged.hu

**Abstract figure legend** Putative mechanism by which diabetes causes increased ductal secretion. The activity of the  $\text{Cl}^-/\text{HCO}_3^-$  exchanger is enhanced in diabetes through the overexpression of ductal acid-base transporters, namely, the cystic fibrosis transmembrane conductance regulator (CFTR), the  $\text{Na}^+/\text{H}^+$  exchanger-1 (NHE-1), anoctamine-1 (ANO-1) and the aquaporin-1 (AQP-1) water channel. Furthermore, high extracellular glucose directly stimulates NHE-1, which may also contribute to increased secretion. Diabetes also causes the upregulation of secretin receptors (SCTRs) at the mRNA level, but the exact role of secretin in the stimulatory effect of diabetes requires further investigations.

### Key points

- There is a lively interaction between the exocrine and endocrine pancreas not only under physiological conditions, but also under pathophysiological conditions
- The most common disease affecting the endocrine part is type-1 diabetes mellitus (T1DM), which is often associated with pancreatic exocrine insufficiency
- Compared with acinar cells, there is considerably less information regarding the effect of diabetes on pancreatic ductal epithelial cells, despite the fact that the large amount of fluid and  $\text{HCO}_3^-$  produced by ductal cells is essential for maintaining normal pancreatic functions
- Ductal fluid and  $\text{HCO}_3^-$  secretion increase in T1DM, in which increased cystic fibrosis transmembrane conductance regulator activation plays a central role.
- We have identified a novel interaction between T1DM and ductal cells. Presumably, the increased ductal secretion represents a defence mechanism in the prevention of diabetes, but further studies are needed to clarify this issue.

### Introduction

The pancreas is a dual gland that performs exocrine and endocrine functions. Although the exocrine and endocrine pancreas are functionally and anatomically separate, there is a lively interaction between them; thus, a disease that affects either part can impact the other

(Gal et al., 2021). The most common disease affecting the endocrine pancreas is diabetes mellitus (DM), which is the result of reduced insulin production or reduced insulin sensitivity. Depending on the underlying cause, DM is categorized as type 1 (T1DM) or type 2 (T2DM). T1DM is an autoimmune disease, in which the body destroys insulin-producing beta cells in the pancreas,

leading to reduced insulin production and ultimately hyperglycaemia. Several clinical and experimental studies have shown that exocrine function is also impaired in T1DM. The lack of insulin decreases the secretion of digestive enzymes, which results in exocrine pancreatic insufficiency (EPI) (Creutzfeldt et al., 2005; Hardt & Ewald, 2011; Hardt et al., 2003; Piciucchi et al., 2015; Radlinger et al., 2020; Zsori et al., 2018). Several factors may be involved in the development of EPI. One of the most accepted is the reduced trophic effect of insulin on acinar cells (Mossner et al., 1984, 1985); however, fibrosis, inflammation and microangiopathy, which develop during long-term diabetes, are probably also involved (Hayden et al., 2008; Rodriguez-Calvo et al., 2014; Zsori et al., 2018). Compared with acinar cells, there is considerably less information regarding the effect of diabetes on pancreatic ductal epithelial cells (PDECs). Although, PDECs comprise only a small proportion of the exocrine pancreas, they have an important physiological role. They secrete a  $\text{HCO}_3^-$ -rich, isotonic fluid which neutralizes the acidic pH entering the duodenum from the stomach, thereby providing optimal pH conditions for digestion. In addition,  $\text{HCO}_3^-$  has an important protective role by neutralizing protons secreted by the acini, thereby preventing the premature activation of digestive enzymes (Behrendorff et al., 2010; Hegyi, Maleth et al., 2011; Hegyi, Pandol et al., 2011). Ductal fluid and  $\text{HCO}_3^-$  secretion are mediated by ion transporters, which are differentially expressed on the luminal and basolateral membranes, resulting in functional polarization of the ductal cells. Among the ion transporters, the apically localized  $\text{Cl}^-/\text{HCO}_3^-$  exchanger and the cystic fibrosis transmembrane conductance regulator (CFTR)  $\text{Cl}^-$  channel have an important role in  $\text{HCO}_3^-$  secretion (Park et al., 2010; Wang et al., 2006); however, little is known with respect to how diabetes affects the function of these transporters and many studies have yielded contradictory results. Futakuchi et al. (2009) showed that high extracellular glucose increases  $\text{Na}^+$  uptake by the sodium-dependent glucose co-transporter-1, which increases intracellular  $\text{Na}^+$  levels and ultimately induces membrane depolarization. Depolarization of the apical membrane reduces the electrochemical driving force for  $\text{Cl}^-$  and  $\text{HCO}_3^-$  efflux, and therefore, impairs fluid and  $\text{HCO}_3^-$  secretion (Futakuchi et al., 2009); however, other studies have found that diabetes increases basal fluid secretion with reduced protein output (Okabayashi, Otsuki, Ohki, Nakamura et al., 1988; Okabayashi, Otsuki, Ohki, Suehiro et al., 1988; Patel et al., 2004). By contrast to basal secretion, secretin-stimulated pancreatic juice flow is significantly reduced in diabetes (Okabayashi, Otsuki, Ohki, Nakamura et al., 1988). Most of these studies are outdated and, because of the conflicting results, it is not clear how diabetes affects ductal functions. Because ductal cells play an essential role in the maintenance of pancreas

integrity, identification of the mechanism through which ductal fluid secretion is altered in diabetes may bring us closer to understanding the pathogenesis of exocrine insufficiency.

In the present study, we determined the effect of diabetes on the activity and expression of the main ductal ion transporters. We used isolated pancreatic ducts from streptozotocin-induced T1DM mice to measure changes in intracellular pH as well as protein and gene expression. We demonstrated that the activity and expression of the main acid–base transporters as well as ductal fluid and  $\text{HCO}_3^-$  secretion was increased in diabetes, in which the CFTR  $\text{Cl}^-$  channel plays a central role.

## Methods

### Ethical approval

Animal experiments were conducted in accordance with the Guide for the Care and Use of Laboratory Animals (Department of Health and Human Services, USA). In addition, the experimental protocol was approved by the local Ethical Board of the University of Szeged, Hungary, and by the Public Health and Food Chain committee, Csongrad County Government Office, Hungary (XI./128/2019).

### Transgenic mice

CFTR knockout (KO) mice on an FVB/N background were kindly provided by Dr Ursula Seidler (Hannover Medical School, Hannover, Germany). The animals were housed in standard plastic cages under a 12:12 h light/dark photoperiod at room temperature ( $23 \pm 1^\circ\text{C}$ ) and had free access to standard or CFTR-specific laboratory chow and drinking solutions. Functional experiments were performed on litter-matched (age 8–12 weeks, male) wild-type (WT) and CFTR KO mice. The mice were genotyped prior to the experiments by isolating genomic DNA from the tail and amplifying by traditional PCR.

### Chemicals and solutions

2,7-Bis-(2-carboxyethyl)-5(6)-carboxyfluorescein acetoxymethyl ester (BCECF-AM) and MQAE [*N*-(ethoxycarbonylmethyl)-6-methoxyquinolinium bromide] were purchased from Invitrogen (Eugene, OR, USA). BCECF-AM (2 mM) and MQAE (1 mM) were prepared in dimethyl sulfoxide and stored at  $-20^\circ\text{C}$ . Chromatographically pure collagenase was purchased from Worthington (Lakewood, NJ, USA). Secretin (SCT) and forskolin were purchased from Tocris (Bristol, UK). The secretin enzyme-linked immunosorbent assay (ELISA) kit was purchased from Biotechne (Minneapolis,

**Table 1. Composition of solutions**

	Standard Hepes	Standard HCO <sub>3</sub> <sup>-</sup>	NH <sub>4</sub> <sup>+</sup> in HCO <sub>3</sub> <sup>-</sup>	Cl <sup>-</sup> -free HCO <sub>3</sub> <sup>-</sup>
NaCl	140	115	95	
KCl	5	5	5	
MgCl <sub>2</sub>	10	1	1	
CaCl <sub>2</sub>	1	1	1	
HEPES	1			
D-glucose	10	10	10	10
NaHCO <sub>3</sub>		25	25	25
NH <sub>4</sub> Cl			20	
Na-gluconate				115
KNO <sub>3</sub>				5
Ca-gluconate				6
Mg-gluconate				1

Values are concentrations (in mM).

MN, USA) and the cholecystokinin (CCK) ELISA kit was purchased from Raybiotech (Peachtree Corners, GA, USA). Cryomatrix, Hoechst33342, anti- $\beta$ -actin antibody (Cat. MA5-15 739) and fluorescence-labelled secondary antibodies (Cat. A-32 723; A-21 244) were obtained from Thermo Scientific (Waltham, MA, USA). Anti-CFTR, anti-NHE1, anti-ANO1 and anti-AQP1 antibodies (Cat. ACL-006; ANX-010; ACL-011; and AQP-001, respectively) were purchased from Alomone Labs (Jerusalem, Israel). Tablets for the protease inhibitor cocktail were purchased from Roche (Budapest, Hungary). All other chemicals were obtained from Merck (Budapest, Hungary). The composition of the solutions used for microfluorimetry and video microscopy measurements are shown in Table 1. A standard Hepes-buffered solution was gassed with 100% O<sub>2</sub> and the pH was adjusted to 7.4 with NaOH. Standard HCO<sub>3</sub><sup>-</sup>/CO<sub>2</sub>-buffered solutions were gassed with a mixture of 95% O<sub>2</sub> and 5% CO<sub>2</sub> and adjusted to a pH of 7.4. All experiments were performed at 37°C.

### Induction of diabetes

To establish a type 1 diabetes model, the protocol of the Diabetic Complications Consortium was used. Briefly, diabetes was induced in 8–12-week-old mice, by daily i.p. administration of 50  $\mu$ g kg<sup>-1</sup> body weight streptozotocin (STZ), dissolved in citrate buffer (pH 4.5), for 5 consecutive days. The mice were fasted for 6 h prior to STZ injection. Control animals received equal amounts of citrate buffer. The development of diabetes was confirmed by measuring fasting blood glucose levels 4 weeks after the first injection. Animals with blood glucose levels >12 mmol L<sup>-1</sup> were considered diabetic. Blood glucose concentrations were determined using a

blood glucose meter (77 Elektronika, Budapest, Hungary). The mice were killed after week 4 by pentobarbital overdose (200 mg kg<sup>-1</sup> body weight i.p.) and exsanguinated through cardiac puncture. The pancreas was immediately removed, trimmed from fat and lymphatic tissue, and a portion was fixed in 6% neutral formaldehyde solution, embedded in paraffin blocks, cut into 3  $\mu$ m thick sections, stained with haematoxylin and eosin, and observed by light microscopy. Small pieces of the pancreas were fixed in 3% glutaraldehyde for transmission electron microscopy. The other portion of the pancreas was used for the isolation of ducts. Blood samples were collected in Microvette CB300 fluoride/heparin-coated capillaries (Sarstedt, Nümbrecht, Germany), centrifuged at 2500 g for 15 min at 4°C, and the plasma was stored at -20°C until use.

### Isolation of pancreatic ducts and measurement of intracellular pH

Intra/interlobular ducts were isolated from the pancreas of WT and CFTR KO mice by enzymatic digestion as previously described (Argent et al., 1986). Changes in intracellular pH (pH<sub>i</sub>) were measured using the pH-sensitive fluorescent dye, BCECF and the microfluorimetric technique. Pancreatic ducts were incubated with 2  $\mu$ M BCECF-AM for 1 h at 37°C then attached to a cover glass. This formed the base of a perfusion chamber, which was mounted on the stage of an IX71 live cell imaging fluorescence microscope (Olympus, Budapest, Hungary). The cells were excited at 440 and 490 nm and emission was monitored at 530 nm. Five to seven regions of interest (ROIs) were marked for each experiment and one measurement per second was obtained. The 490/440 fluorescence ratio was calibrated to pH<sub>i</sub> using the high K<sup>+</sup>-nigericin technique as previously described (Hegyi et al., 2004; Thomas et al., 1979).

### Measurement of HCO<sub>3</sub><sup>-</sup> secretion

To estimate HCO<sub>3</sub><sup>-</sup> efflux, the activity of the Cl<sup>-</sup>/HCO<sub>3</sub><sup>-</sup> exchanger was measured by the NH<sub>4</sub>Cl pre-pulse technique and the Cl<sup>-</sup> withdrawal technique. For the NH<sub>4</sub>Cl pre-pulse technique, ducts were exposed to 20 mM NH<sub>4</sub>Cl in HCO<sub>3</sub><sup>-</sup>/CO<sub>2</sub>-buffered solution, which resulted in an immediate increase in pH<sub>i</sub> resulting from the influx of NH<sub>3</sub> across the membrane. After maximal alkalization, the pH<sub>i</sub> began to recover. Under these conditions, the initial rate of pH<sub>i</sub> ( $\Delta$ pH/ $\Delta$ t) recovery (over the first 30 s) reflects the rate of HCO<sub>3</sub><sup>-</sup> secretion (base efflux) (Hegyi et al., 2003; Hegyi et al., 2005). After the removal of NH<sub>4</sub>Cl, the pH<sub>i</sub> suddenly decreased because of the dissociation of intracellular NH<sub>4</sub><sup>+</sup> to H<sup>+</sup> and NH<sub>3</sub>. In HCO<sub>3</sub><sup>-</sup>/CO<sub>2</sub>-buffered solution, the initial rate of recovery from the acid load (over the

first 60 s) reflects the activity of  $\text{Na}^+/\text{H}^+$  exchangers (NHEs) and the  $\text{Na}^+/\text{HCO}_3^-$  cotransporter (NBC). For the  $\text{Cl}^-$  withdrawal technique,  $\text{Cl}^-$  was removed from the external solution that caused a sudden alkalization of the  $\text{pH}_i$  resulting from the reverse operation of the  $\text{Cl}^-/\text{HCO}_3^-$  exchanger. The initial rate of alkalization (over the first 60 s) or the rate of recovery from alkalosis (over the first 60 s) reflects the activity of the exchanger. Transmembrane base flux  $[(J(B^-))]$  was calculated using:  $J(B^-) = \Delta\text{pH}/\Delta t \times \beta_{\text{total}}$ , where  $\Delta\text{pH}/\Delta t$  is the initial rate of recovery and  $\beta_{\text{total}}$  is the total buffering capacity (Hegyí et al., 2003; Weintraub & Machen, 1989).

### Measurement of CFTR activity

CFTR activity was analysed by measuring the intracellular  $\text{Cl}^-$  concentration using MQAE fluorescent dye and forskolin. The fluorescence intensity of MQAE is inversely proportional to  $\text{Cl}^-$  because of its quenching effect on the dye. Pancreatic ducts were incubated with MQAE ( $5 \mu\text{M}$ ) for 1 h at  $37^\circ\text{C}$ , then perfused with  $\text{HCO}_3^-/\text{CO}_2$ -buffered solution containing  $20 \mu\text{M}$  forskolin. Excitation was set to 350 nm and emission was monitored at 510 nm. Five to seven ROIs were marked for each experiment and one measurement per second was obtained. The readings were displayed as fluorescence ratio ( $F/F_0$ ) and a linear trend line was plotted on the curve for the first 2 min (120 s) of forskolin stimulation. The area under the plotted curve was calculated using the definite integral of the equation.

### Measurement of pancreatic fluid secretion

To estimate the rate of ductal fluid secretion, we measured the swelling of the intra-interlobular ducts using the video microscopy technique described previously (Fernandez-Salazar et al., 2004). Briefly, intra-interlobular pancreatic ducts were attached to the cover glass of a perfusion chamber and mounted on the stage of an IX71 live cell imaging fluorescence microscope. To stimulate fluid secretion, the ducts were perfused with forskolin ( $5 \mu\text{M}$ ) and low magnification, bright-field images were captured at intervals of 1 min using a CCD camera (Hamamatsu ORCA-ER; Olympus). The integrity of the ductal wall was confirmed at the end of each experiment using a hypotonic solution. Changes in relative luminal volume were analysed using Image J software (Fernandez-Salazar et al., 2004; Pascua et al., 2009).

Pancreatic fluid secretion was also assessed *in vivo* as previously described (Perides et al., 2010). Briefly, mice were anaesthetized with the combination of ketamine ( $100 \text{ mg kg}^{-1}$  i.p.) and xylazine ( $12.5 \text{ mg kg}^{-1}$  i.p.) and, for pain relief, a single buprenorphine ( $0.1 \text{ mg kg}^{-1}$  i.p.) injection was administered. To maintain body temperature, animals were kept on a heating pad ( $37^\circ\text{C}$ )

during the entire experiment. After median laparotomy, the lumen of the common biliopancreatic duct was cannulated using a 30-gauge needle with filed ends. To prevent contamination with bile, the ductus hepaticus was occluded with a microvessel clip. Pancreatic fluid secretion was stimulated by i.p. administration of secretin ( $1 \text{ CU kg}^{-1}$ ) and the pancreatic juice was collected through a polyethylene tube over 60 min.

### Immunohistochemistry

Isolated pancreatic ducts were embedded in cryomatrix, snap-frozen in liquid nitrogen, and cut into  $10 \mu\text{m}$  thick sections. Immunofluorescence labelling was performed based on the protocol provided at [www.novusbio.com](http://www.novusbio.com). Briefly, tissue sections were fixed with 4% para-formaldehyde in phosphate-buffered saline (PBS) for 15 min and permeabilized by washing twice with PBS containing 1% goat serum (GS) and 0.4% Triton X-100 for 10 min. Blocking was carried out for 30 min in PBS-Tween 20 containing 5% GS, followed by incubation with primary antibodies overnight on  $4^\circ\text{C}$ . The sections were then incubated with Hoechst 33342 for 15 min followed by a washing step and incubation with secondary antibodies for 1 h. After a washing step, the sections were covered with Fluoromount mounting medium (Sigma, St Louis, MO, USA) and allowed to dry for 12 h under aluminium foil. Primary ( $2 \mu\text{g mL}^{-1}$  for CFTR, ANO1 and NHE-1 antibodies;  $2.5 \mu\text{g mL}^{-1}$  for anti-AQP1;  $4 \mu\text{g mL}^{-1}$  for anti- $\beta$ -actin) and secondary ( $5 \mu\text{g mL}^{-1}$  for goat anti-rabbit Alexa Fluor 647;  $8 \mu\text{g mL}^{-1}$  for goat anti-mouse Alexa Fluor 488) antibodies and Hoechst 33 342 ( $20 \mu\text{g mL}^{-1}$ ) were diluted in PBS supplemented with 1% GS. All steps were carried out at room temperature unless specified otherwise. Images were captured using an LSM 880 confocal microscope (Carl Zeiss Technika Kft, Budaörs, Hungary). An optimal pinhole size and laser intensity was defined for every target antigen and the same settings were used to record all samples.

### Quantitation of immunostainings

The images were evaluated using ImageJ (NIH, Bethesda, MD, USA). The measured area was restricted to the layer of epithelial cells and to a constant threshold value of intensity. The average intensity in the green and red channels was then determined. Red intensity values marking the antigens of interest were normalized to the green intensity values representing  $\beta$ -actin.

### Real-time PCR (RT-PCR)

Intra-interlobular pancreatic ducts were isolated from six normal and six diabetic mice and pooled for total RNA

**Table 2. Taqman assays used for the investigation of ion transporter expression**

Gene symbol	Official full name	GenBank ref. no.	Taqman assay ID
<i>CFTR</i>	Cystic fibrosis transmembrane conductance regulator	NC_000072	Mm00445197_m1
<i>ANO-1</i> or <i>TMEM16A</i>	Anoctamin-1	NC_000073.7	Mm00724407_m1
<i>AQP-1</i>	Aquaporin-1	NC_000072.7	Mm01326466_m1
<i>AQP-5</i>	Aquaporin-5	NC_000081.7	Mm00437578_m1
<i>AQP-8</i>	Aquaporin-8	NC_000073.7	Mm00431846_m1
<i>Slc9a1</i>	Solute carrier family 9 (Na <sup>+</sup> /H <sup>+</sup> exchanger) member A1	NC_000001.11	Mm00444270_m1
<i>Slc9a2</i>	Solute carrier family 9 (Na <sup>+</sup> /H <sup>+</sup> exchanger) member A2	NC_000067.7	Mm01237129_m1
<i>Slc26a3</i> ( <i>DRA</i> )	Solute carrier family 26 (Cl <sup>-</sup> /HCO <sub>3</sub> <sup>-</sup> exchanger), member 3	NC_000078.7	Mm00445313_m1
<i>Slc26a6</i> ( <i>PAT-1</i> )	Solute carrier family 26 (Cl <sup>-</sup> /HCO <sub>3</sub> <sup>-</sup> exchanger), member 6	NC_000075.7	Mm00506742_m1
<i>Slc4a4</i>	Solute carrier family 4 (Na <sup>+</sup> /HCO <sub>3</sub> <sup>-</sup> co-transporter), member 4	NC_000071.7	Mm01347935_m1

extraction with a NucleoSpin RNA Kit (Macherey-Nagel, Düren, Germany) in accordance with the manufacturer's instructions. Total RNA (2 µg) was reverse-transcribed using the High-Capacity cDNA Reverse Transcription Kit (Applied Biosystems, Foster City, CA, USA). RT-PCR was performed on a Light Cycler 96 instrument (Roche Magyarország Kft, Budaörs, Hungary) using TaqMan probe sets for specific genes (Thermo Fisher Scientific, Darmstadt, Germany). Quantitative RT-PCR reactions were performed as previously described (Laczko et al., 2016). The results were expressed as fold-changes calculated by the  $2^{-\Delta\Delta CT}$  method. Genes with expression values  $\leq 0.5$  were considered downregulated, whereas values  $\geq 2$  were considered upregulated. Values ranging from 0.51 to 1.99 were not considered to be significant. Table 2 provides information regarding the TaqMan assays.

### Transmission electron microscopy

For post-embedding transmission electron microscopy, small pieces of the pancreas were fixed in 3% glutaraldehyde. The tissues were rinsed with PBS and further fixed for 1 h in 2% OsO<sub>4</sub>. The samples were then dehydrated in increasing concentrations of ethanol, rinsed with uranyl acetate and acetone, and embedded in Embed 812 (Electron Microscopy Sciences, Hatfield, PA, USA). The embedded blocks were used to prepare ultrathin (70 nm) sections (Ultracut S ultra-microtome; Leica, Wetzlar, Germany), which were mounted on copper grids. The grids were counterstained with uranyl acetate and lead citrate (Merck Millipore, Darmstadt, Germany) and examined and imaged using a JEOL JEM

1400 transmission electron microscope (JEOL, Tokyo, Japan). Five digital photographs of the cells were captured at magnifications of 5000× and 8000× using TEM Centre software (JEOL).

### ELISA

Plasma samples obtained by cardiac puncture were transferred to fluoride/heparin-coated capillaries and centrifuged at 2500 × *g* for 20 min at 4°C. The samples were stored at -20°C and thawed on ice before use. Pancreas homogenates were prepared by grinding 100 mg of tissue in liquid nitrogen using a mortar and pestle and dissolving it in 1 mL of ice-cold protease inhibitor cocktail. The SCT and CCK assays were performed following based on the manufacturer's instructions.

### Statistical analysis

Prism, version 9.5.1 (GraphPad Software Inc., San Diego, CA, USA) was used to produce graphs and images. Data are presented as the mean ± SD and box and whisker plots showing the median, quartiles and extremes. Shapiro-Wilk and Kolmogorov-Smirnov tests were used to analyse data distribution. The equality of variances was analysed using an *F* test. One-way ANOVA (with Tukey's multiple comparisons test), Student's *t* test (with Welch's correction as needed), the Kruskal-Wallis test (with Dunn's multiple comparisons test) and the Mann-Whitney test were used to determine statistical significance.

## Results

### Morphology of the exocrine pancreas in diabetes

T1DM caused a decrease in the number and size of islets by the destruction of insulin-producing beta cells (Fig. 1A). In addition, characteristics of chronic pancreatitis, such as fibrosis, acinar atrophy and leukocyte infiltration, were also observed at low levels. By contrast, the structure of the ducts was preserved. Electron microscopic examination of the pancreas showed enlarged mitochondria and a fragmented mitochondrial internal membrane structure in the acini (Fig. 1B). Enlargement of the mitochondria was also observed in ducts and islets, but to a much lesser extent compared with the acini.

### Pancreatic ductal fluid secretion increases in diabetes

The volume of fluid secreted by ductal cells is an important indicator of ductal function. Therefore, the rate of fluid secretion was determined under *in vitro* and *in vivo* conditions. For the *in vitro* measurements, the rate of fluid secretion was estimated from the volume change of the isolated ductal fragments (Fig. 2A and B). Following forskolin stimulation, the amount of fluid secreted by the diabetic ducts was significantly higher compared to that of non-diabetic ducts ( $13.2 \pm 2.14$  vs.  $9.29 \pm 0.51\%$ ). *In vivo* fluid secretion studies revealed similar results to that observed *in vitro*. Both basal and secretin-stimulated ( $1 \text{ CU kg}^{-1}$ ) fluid secretion were significantly increased in diabetic mice compared with normal mice ( $0.73 \pm 0.12$  vs.  $1.15 \pm 0.08 \mu\text{L h}^{-1} \text{ g}^{-1}$  body weight basal secretion and  $1.48 \pm 0.24$  vs.  $2.48 \pm 0.25 \mu\text{L h}^{-1} \text{ g}^{-1}$  body weight stimulated secretion) (Fig. 2C).

### Diabetes increases the activity and expression of ductal acid–base transporters

Intra-interlobular ducts were isolated from normal and diabetic mice and the alkaline load method was used to measure the activity of acid–base transporters in the ductal cells. In previous studies, we found that the degree of regeneration from alkalosis in  $\text{HCO}_3^-/\text{CO}_2$ -containing extracellular solution reflects the activity of the  $\text{Cl}^-/\text{HCO}_3^-$  exchanger, whereas the regeneration from acidosis indicates the activity of the NHE and the NBC (Hegyí et al., 2003). Both alkali and acid regeneration were increased in diabetic mice compared with control mice [rate of alkali regeneration:  $3.2 \pm 0.09$  vs.  $4.86 \pm 0.14 -J(B^- \text{ min}^{-1})$ ; rate of acid regeneration  $7.25 \pm 0.3$  vs.  $11.45 \pm 0.34 -J(B^- \text{ min}^{-1})$ ], indicating that diabetes increases the activity of these transporters (Fig. 3Aa–Ac). To confirm this result, the  $\text{Cl}^-$  withdrawal method was used (Fig. 3Ba–Bc). The removal of extracellular  $\text{Cl}^-$  in the presence of  $\text{HCO}_3^-$  induces

a robust alkalosis, because of the reverse mode of the exchanger. During the re-administration of extracellular  $\text{Cl}^-$ , the  $\text{pH}_i$  is regenerated and the rate of regeneration reflects the activity of the  $\text{Cl}^-/\text{HCO}_3^-$  exchanger. Similar to the alkali-load method, the activity of the exchanger was also enhanced during diabetes (Fig. 3Bb), although no differences in  $\text{pH}_i$  were observed (Fig. 3Bc).

Next, we examined mRNA and protein expression of the major acid–base transporters using RT-PCR and immunohistochemistry. Intra-interlobular pancreatic ducts were isolated from normal and diabetic mice and the expression of CFTR, anoctamine-1 (ANO-1), NHEs (NHE-1 and NHE2),  $\text{Cl}^-/\text{HCO}_3^-$  exchangers (Slc26a3 and Slc26a6), NBC and aquaporins (AQP1, AQP5 and AQP8) was measured (Fig. 4A). Among the transporters, the expression of CFTR, ANO-1, NHE-1 and AQP-1 mRNA was significantly increased in diabetes; however, no differences were observed in the expression of the other transporters. The results obtained by PCR were also confirmed at the protein level (Fig. 4B and C). Using immunostaining, we confirmed the increased protein expression of CFTR, ANO-1, NHE-1 and AQP-1 in diabetic mice.

### The central role of CFTR in diabetes-induced $\text{HCO}_3^-$ secretion

The CFTR  $\text{Cl}^-$  channel plays an essential role in ductal  $\text{HCO}_3^-$  secretion. Its expression also increases in diabetes; thus, we considered how the activity of the channel changes under diabetic conditions. To estimate the activity of the channel, the  $\text{Cl}^-$ -sensitive fluorescent dye, MQAE, and the specific CFTR activator, forskolin, were used (Fig. 5A and B). Administration of  $20 \mu\text{M}$  forskolin increased  $\text{Cl}^-$  efflux in the normal and diabetic mice; however, the increase was significantly higher in diabetes.

To confirm the role of CFTR in diabetes-induced  $\text{HCO}_3^-$  secretion, we examined the activity of the  $\text{Cl}^-/\text{HCO}_3^-$  exchanger in the absence of CFTR, using CFTR knockout mice. Diabetes was induced in both wild-type (WT) and CFTR KO mice, and the activity of the exchanger was assessed by the alkali-load technique (Fig. 6A). In the absence of CFTR, the rate of  $\text{HCO}_3^-$  secretion was significantly reduced compared to the WT mice [ $3.2 \pm 0.09$  vs.  $2.27 \pm 0.1 -J(B^- \text{ min}^{-1})$ ]. KO mice with induced diabetes also exhibited increased  $\text{HCO}_3^-$  secretion rates compared with their non-diabetic counterparts [ $3.01 \pm 0.08$  vs.  $2.27 \pm 0.1 -J(B^- \text{ min}^{-1})$ ]; however, this increment fell short compared to that observed between diabetic and non-diabetic WT mice [ $3.01 \pm 0.08$  vs.  $4.86 \pm 0.14 -J(B^- \text{ min}^{-1})$ ] and did not reach statistical significance. Interestingly, no difference was observed in the rate of regeneration from acidosis between WT and KO mice; however, in the absence of

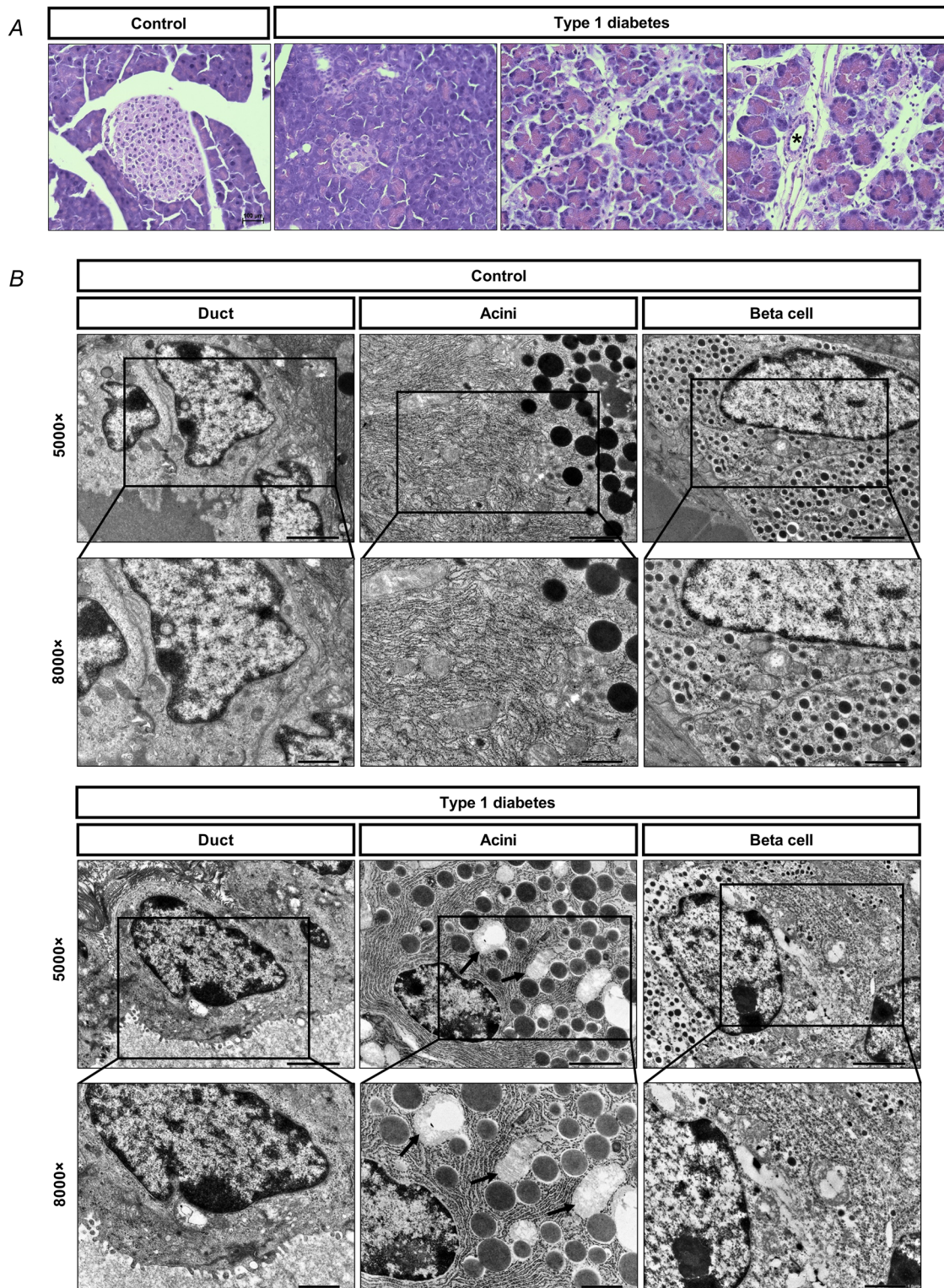


**Figure 1. Effect of diabetes on pancreas morphology**

*A*, haematoxylin and eosin staining of the pancreas from normal and type-1 diabetic mice. An asterisk shows the pancreatic duct. Scale bar = 100  $\mu\text{m}$ . *B*, representative electron micrograph images of pancreatic duct, acini, and  $\beta$  cells from control and type-1 diabetic mice. Black arrows on the upper (magnification, 5000 $\times$ ) and lower (magnification, 8000 $\times$ ) panels indicate mitochondria.

CFTR, the diabetes-induced activity of NHE and/or NBC was significantly decreased [ $11.4 \pm 0.34$  vs.  $9.4 \pm 0.32$   $J(B^{-1} \text{ min}^{-1})$ ] (Fig. 6B).

In the absence of CFTR, the rate of fluid secretion was far below that of WT mice ( $0.53 \pm 0.08$  vs.  $1.19 \pm 0.06$   $\mu\text{L h}^{-1} \text{g}^{-1}$ ) (Fig. 6C). The presence of diabetes slightly increased the amount of fluid secretion in CFTR KO mice ( $0.84 \pm 0.05$  vs.  $0.53 \pm 0.17$   $\mu\text{L h}^{-1} \text{g}^{-1}$ ), but did not result in a significant difference. Taken together, these results indicate that CFTR plays an important role in diabetes-induced, increased fluid and  $\text{HCO}_3^-$  secretion.

### Effects of high glucose on the activity of acid-base transporters

The mechanism through which the functioning of transporters is increased in diabetes was examined. T1DM is often associated with hyperglycaemia; therefore, we determined the effect of acute and chronic glucose

treatment on the activity of the transporters using the previously described alkali-load technique. During acute treatment, the isolated ducts were perfused with standard  $\text{HCO}_3^-/\text{CO}_2$  solution containing 44.4 mM glucose, 8 min before the ammonia pulse, during the ammonia pulse, and 8 min after the ammonia pulse. During chronic treatment, the ducts were incubated in culture media supplemented with 44.4 mM glucose overnight. Upon acute glucose administration, no difference was observed in the rate of regeneration from alkalosis or acidosis between normal and diabetic mice (Fig. 7Aa and Ab). Similarly, chronic treatment did not affect the rate of regeneration from alkalosis, but increased the recovery from acidosis, indicating that the activity of NHE and/or NBC increases in response to chronic high glucose (Fig. 7Ab). The activity of the  $\text{Cl}^-/\text{HCO}_3^-$  exchanger was also examined using the  $\text{Cl}^-$  withdrawal technique; however, neither the acute, nor the chronic high glucose treatment caused any change in activity (Fig. 7Ba) or change in the maximal  $\text{pH}_i$  (Fig. 7Bb).

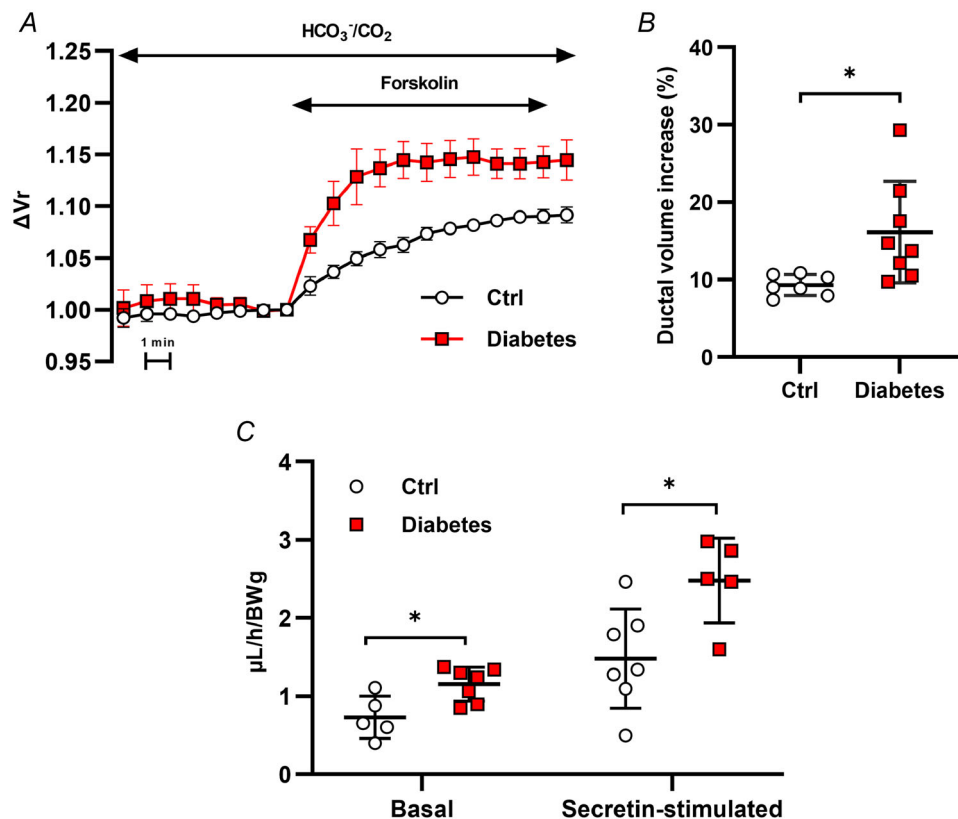


**Figure 2. Effect of diabetes on ductal fluid secretion**

A, pancreatic ductal fluid secretion was measured on intact pancreatic ducts isolated from control and diabetic mice. Swelling of pancreatic ducts was measured using video microscopy and analysed using Image J. B, ductal volume increase was measured during forskolin ( $5 \mu\text{M}$ ) stimulation (between 8 and 18 time points) and expressed as a percentage. Data are shown as the mean  $\pm$  SD ( $n = 7\text{--}8$  ducts/three mice/groups).  $*P = 0.021$  vs. Control using Welch's  $t$  test. C, bar chart showing the rate of *in vivo* pancreatic fluid secretion under basal and secretin-stimulated ( $1 \text{ CU kg}^{-1}$ ) conditions in control and diabetic mice. Data are shown as the mean  $\pm$  SD ( $n = 5\text{--}7$  mice/groups).  $*P = 0.013$  (basal secretion) and  $0.0174$  (secretin-stimulated secretion) vs. Control, using an unpaired  $t$  test.

### Serum levels of secretin and cholecystinin in diabetic mice

To determine whether hormonal effects are involved in the increased secretion, we measured serum secretin and CCK levels in the diabetic mice. The primary physiological function of secretin is to stimulate the secretion of  $\text{HCO}_3^-$ -rich pancreatic fluid, whereas CCK promotes the release of digestive enzymes. Neither serum secretin, nor serum CCK levels were different between the control and diabetic mice (Fig. 8A and B). Secretin was also examined in pancreatic homogenate (Fig. 8C) and we observed a slight increase in diabetic animals, although this was not significant. Finally, we examined whether there was a difference in the amount of ductal

secretin receptors (SCTR) (Fig. 8D). RT-PCR revealed that the expression of SCTRs was significantly increased in the intra-interlobular ducts isolated from diabetic mice compared to the ducts isolated from control mice. Protein expression of SCTR also increased in the diabetic ducts, although this was not significant (Fig. 8E and F).

### Discussion

Diabetes has long-term effects on exocrine function; however, less is known about the underlying mechanisms, particularly with respect to ductal cells. In the present study, we showed that the fluid and  $\text{HCO}_3^-$  secretion of ductal cells increased as a result of diabetes, in which

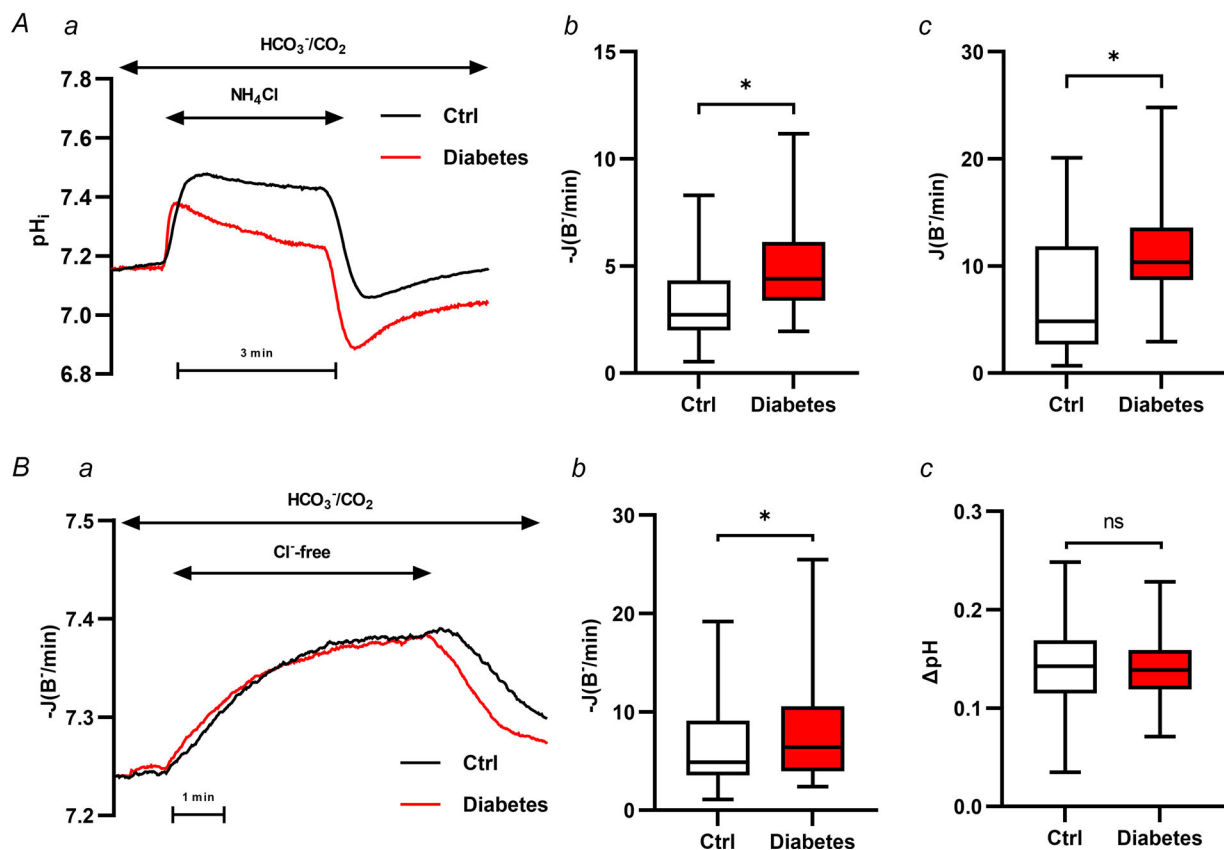


**Figure 3.** Effect of diabetes on the activity of ion transporters from isolated mice pancreatic ducts

A, ion transporter activity was examined using the  $\text{NH}_4\text{Cl}$  pre-pulse technique. Aa, representative pH<sub>i</sub> traces showing the effect of diabetes (red line) on the activity of acid–base transporters in  $\text{HCO}_3^-/\text{CO}_2$ -buffered solution. The rate of regeneration from alkalosis (Ab) reflects the activity of the  $\text{Cl}^-/\text{HCO}_3^-$  exchanger, whereas regeneration from acidosis (Ac) reflects the activity of the  $\text{Na}^+/\text{H}^+$  exchanger and the  $\text{Na}^+/\text{HCO}_3^-$  cotransporter.  $-J(\text{B}^- \text{ min}^{-1})$  and  $J(\text{B}^- \text{ min}^{-1})$  were calculated from the  $\Delta\text{pH}/\Delta t$  obtained by a linear regression analysis of pH<sub>i</sub> measurements made over the first 30 or 60 s, respectively ( $n = 172\text{--}274$  ROIs/14–24 ducts/4–5 mice/groups). \* $P < 0.0001$  vs. Control using the Mann–Whitney test. B, activity of the  $\text{Cl}^-/\text{HCO}_3^-$  exchanger was measured using the  $\text{Cl}^-$  withdrawal technique. Ba, representative pH<sub>i</sub> traces show the effect of extracellular  $\text{Cl}^-$  removal on control (black line) and diabetic (red line) pancreatic ducts in  $\text{HCO}_3^-/\text{CO}_2$ -buffered solution. Box and whisker plots show the rate of regeneration from alkalosis after re-administration of extracellular  $\text{Cl}^-$  (Bb) and the maximal pH<sub>i</sub> change (Bc).  $-J(\text{B}^- \text{ min}^{-1})$  was calculated from the  $\Delta\text{pH}/\Delta t$  obtained by linear regression analysis of pH<sub>i</sub> measurements made over the first 60 s ( $n = 219\text{--}230$  ROIs/21 ducts/4 mice/groups). \* $P = 0.0002$  vs. Control using the Mann–Whitney test. ns:  $P = 0.2687$  vs. Control using Welch's  $t$  test.

increased activation and expression of CFTR and NHE-1 plays a key role.

First, we examined how T1DM affects the morphology of the exocrine and endocrine pancreas using electron microscopy. Acinar cells were identified by the presence of large, dark secretory granules and abundant endoplasmic reticulum and mitochondria. Islets were distinguished by the presence of cell clustering, smaller secretory granules and less endoplasmic reticulum. Although

ductal cells typically have large nuclei, the cells enclose a lumen and cilia are present on the apical membrane of the cells. The most characteristic difference between the normal and diabetic pancreas is the morphological change of mitochondria in acinar cells. In diabetes, the mitochondria were less elongated and more round in shape. In addition, enlargement of the mitochondria and disruption of the inner membrane structure were also observed. Similar results were observed in the

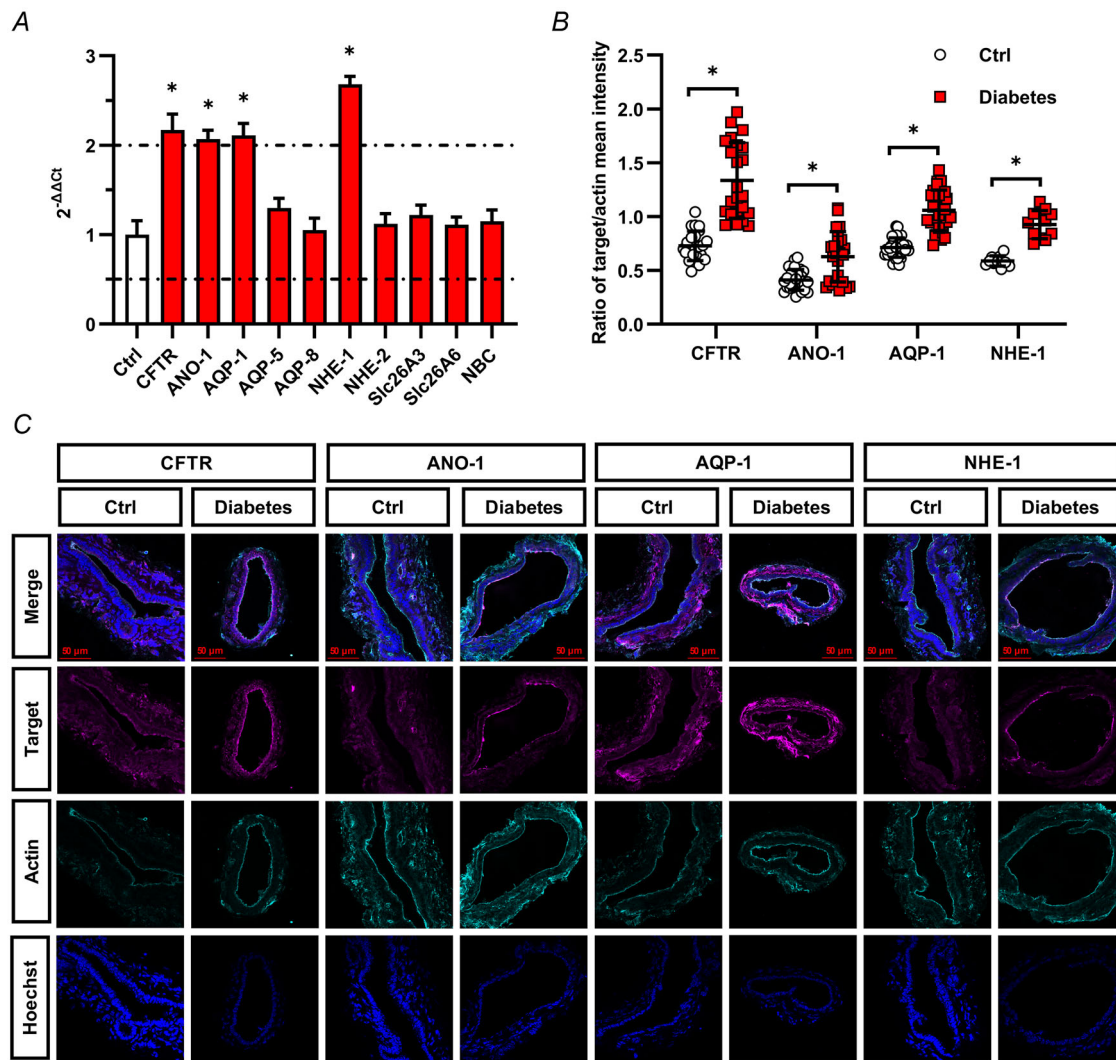


**Figure 4. Effect of diabetes on the mRNA and protein expression of pancreatic ductal ion transporters** Intra-interlobular pancreatic ducts were isolated from control and diabetic mice and the mRNA (A) and protein (B and C) expression of the acid–base transporters was measured by RT-PCR and immunostaining, respectively. A, genes with expression values  $\leq 0.5$  were considered to be downregulated, whereas values  $\geq 2$  were considered to be upregulated. B, quantification of the fluorescence signals was carried out using ImageJ as described in the Methods. Data are shown as the mean  $\pm$  SD. CFTR, cystic fibrosis transmembrane conductance regulator ( $n = 23$  ROIs/8 ducts/4 mice/groups).  $*P < 0.0001$  vs. Control using Welch's  $t$  test. ANO-1, anoctamine-1 ( $n = 24$ – $26$  ROIs/6–7 ducts/3 mice/groups).  $*P < 0.0001$  vs. Control using Welch's  $t$  test. AQP-1, aquaporin-1 ( $n = 30$ – $31$  ROIs/8–9 ducts/3 mice/groups).  $*P = 0.0001$  vs. Control using Welch's  $t$  test. NHE-1,  $\text{Na}^+/\text{H}^+$  exchanger-1 ( $n = 11$  ROIs/3 ducts/2 mice/groups).  $*P < 0.0001$  vs. Control using Welch's  $t$  test. C, representative immunofluorescence staining of pancreatic ducts showing the expression of CFTR, ANO-1, AQP-1, and NHE-1 in control and diabetic ducts.

intermediate cells of T1DM patients (de Boer et al., 2020) and in the beta cells of T2DM patients (Anello et al., 2005). By contrast to acini, ductal mitochondria remained mostly intact. Because mitochondria play an important role in maintaining the normal energy production and balance of the cells, it is possible that

mitochondrial damage occurring in acini contributes to the development of EPI. Meanwhile, the morphology of ductal cells remained largely unaltered, which suggests that ductal functions are preserved in T1DM.

The pancreatic ductal epithelium has a secretory function and produces a  $\text{HCO}_3^-$ -rich luminal fluid. This

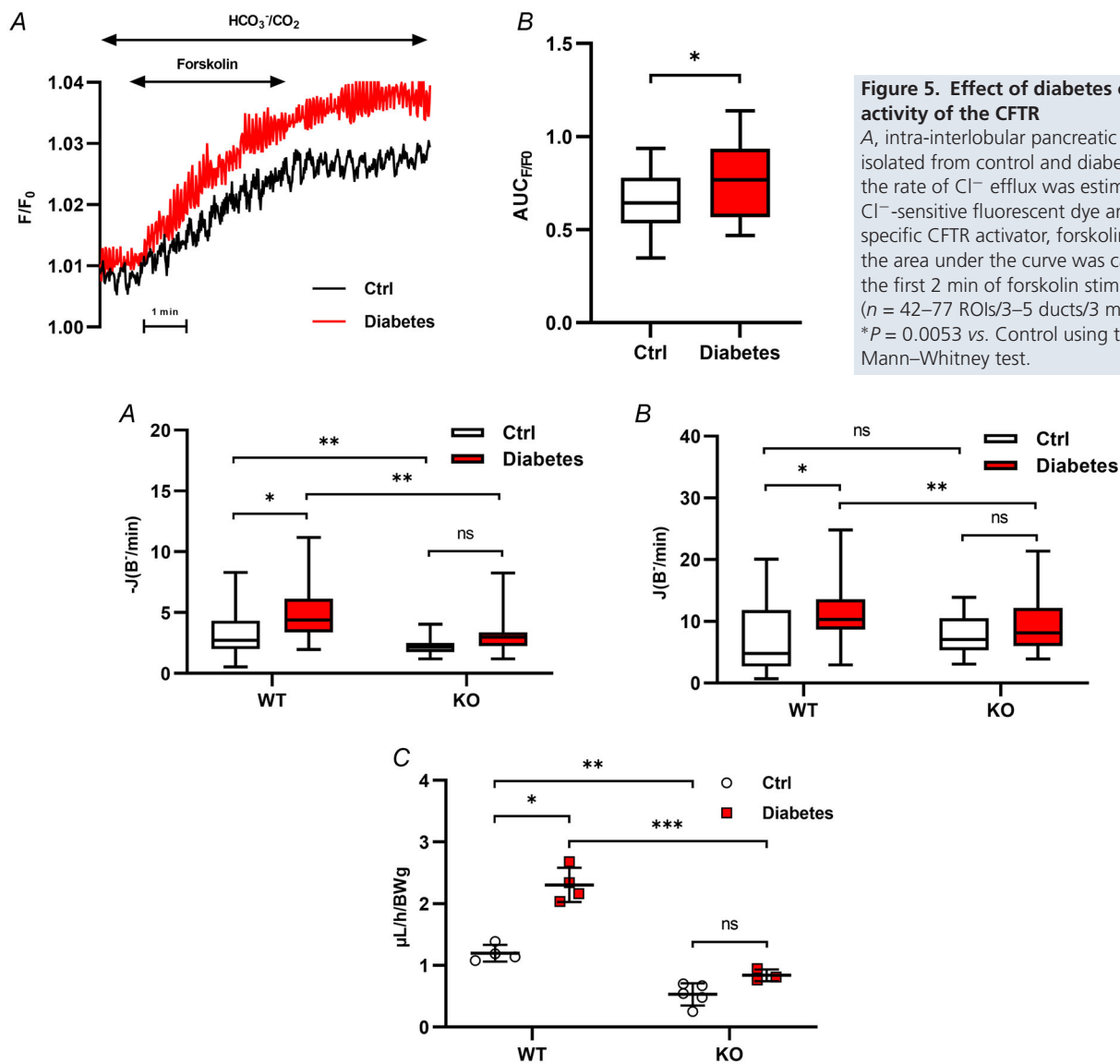


**Figure 5. Effect of diabetes on the activity of the CFTR**

A, intra-interlobular pancreatic ducts were isolated from control and diabetic mice and the rate of  $\text{Cl}^-$  efflux was estimated using a  $\text{Cl}^-$ -sensitive fluorescent dye and the specific CFTR activator, forskolin ( $20 \mu\text{M}$ ). B, the area under the curve was calculated for the first 2 min of forskolin stimulation ( $n = 42\text{--}77$  ROIs/3–5 ducts/3 mice/groups). \* $P = 0.0053$  vs. Control using the Mann–Whitney test.

**Figure 6. Role of the CFTR in diabetes**

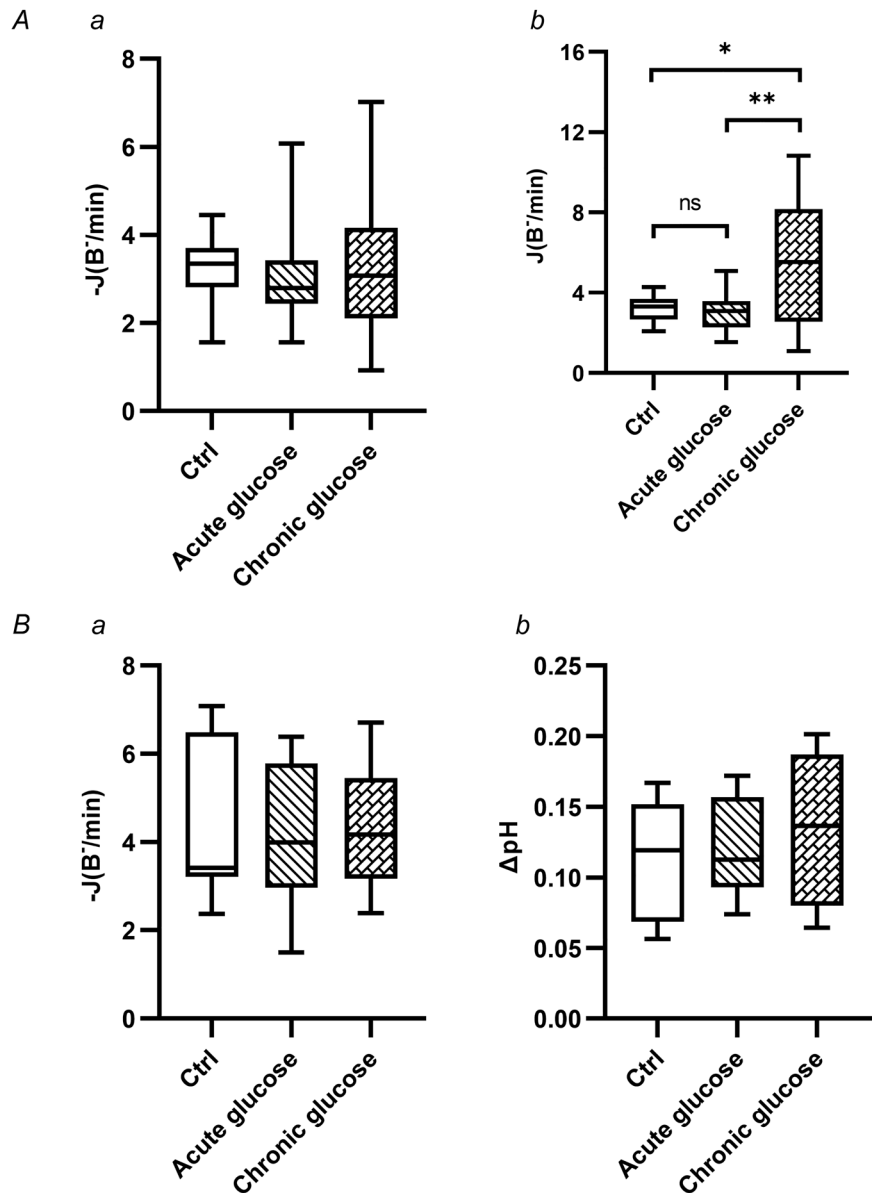
Intra-interlobular pancreatic ducts were isolated from wild-type (WT) and CFTR knockout (KO) mice with or without diabetes and the activity of the acid–base transporters was measured by the  $\text{NH}_4\text{Cl}$  pre-pulse technique in  $\text{HCO}_3^-/\text{CO}_2$ -buffered solution. The rate of regeneration from alkalosis (A) reflects the activity of the  $\text{Cl}^-/\text{HCO}_3^-$  exchanger, whereas regeneration from acidosis (B) reflects the activity of the  $\text{Na}^+/\text{H}^+$  exchanger and the  $\text{Na}^+/\text{HCO}_3^-$  cotransporter.  $-J(\text{B} \cdot \text{min}^{-1})$  and  $J(\text{B} \cdot \text{min}^{-1})$  were calculated from the  $\Delta\text{pH}/\Delta t$  obtained by linear regression analysis of the  $\text{pH}_i$  measurements made over the first 30 or 60 s, respectively. Data are shown as the mean  $\pm$  SD ( $n = 60\text{--}160$  ROIs/5–13 ducts/3 mice/groups). \* $P < 0.0001$  vs. Control, \*\* $P \leq 0.0001$  vs. WT using the Kruskal–Wallis test. In the case of regeneration from alkalosis, ns:  $P = 0.118$  vs. KO/Control. In the case of regeneration from acidosis, ns:  $P = 0.9799$  vs. WT/Control and ns:  $P = 0.2723$  vs. KO/Control. C, scatter plot showing the rate of *in vivo* pancreatic fluid secretion under secretin-stimulated ( $1 \text{ CU kg}^{-1}$ ) conditions in WT and CFTR KO mice with or without diabetes. Data are shown as the mean  $\pm$  SD ( $n = 3\text{--}5$  mice/groups). \* $P < 0.0001$  vs. Control, \*\* $P = 0.011$  vs. WT, \*\*\* $P < 0.0001$  vs. WT, using one-way ANOVA. ns:  $P = 0.1692$  vs. KO/Control.

fluid provides a carrier for the transport of digestive enzymes and counteracts the acid produced by the stomach and acini. Using *in vivo* and *in vitro* approaches, we demonstrated that the amount of pancreatic fluid was significantly increased in streptozotocin-induced T1DM mice. The elevated fluid secretion was observed under basal and secretin-stimulated conditions. The rate of fluid secretion primarily depends on the rate of  $\text{HCO}_3^-$  secretion, and therefore on the activity of ductal ion transporters. The major route for  $\text{HCO}_3^-$  secretion in the ductal cells is the apically localized  $\text{Cl}^-/\text{HCO}_3^-$  exchanger Slc26a6, which mediates the electrogenic exchange of 1  $\text{Cl}^-$  and 2  $\text{HCO}_3^-$  (Shcheynikov et al., 2006). Using the alkali-load method, we found that the activity of the  $\text{Cl}^-/\text{HCO}_3^-$  exchanger increased in

diabetes, which was also confirmed by the  $\text{Cl}^-$  withdrawal technique. In the  $\text{Cl}^-$  withdrawal technique, removal of extracellular  $\text{Cl}^-$  causes a sudden alkalization because of the altered function of the exchanger. In the absence of  $\text{Cl}^-$ , the exchanger operates in reverse mode and absorbs  $\text{HCO}_3^-$  in exchange for  $\text{Cl}^-$ . The absorbed  $\text{HCO}_3^-$  binds free protons and induces alkalosis in the cell. Therefore, this technique allows for the direct measurement of exchanger activity. Interestingly, there was no difference in the degree of alkalosis, nor in the maximum pH change between the control and the diabetic ducts, which suggests that diabetes does not affect the function of the exchanger in reverse mode. Because the CFTR  $\text{Cl}^-$  channel and the  $\text{Cl}^-/\text{HCO}_3^-$  exchanger work closely with one another, we measured

**Figure 7. Effect of extracellular glucose on the activity of ion transporters from isolated mouse pancreatic ducts**

Intra-interlobular pancreatic ducts isolated from control mice were incubated with 44.4 mM glucose during the ammonia pulse (acute treatment) or overnight (chronic treatment). A, activity of the ion transporters was measured using the  $\text{NH}_4\text{Cl}$  pre-pulse technique. The rate of regeneration from alkalosis (Aa) reflects the activity of the  $\text{Cl}^-/\text{HCO}_3^-$  exchanger, whereas regeneration from acidosis (Ab) reflects the activity of the  $\text{Na}^+/\text{H}^+$  exchanger and the  $\text{Na}^+/\text{HCO}_3^-$  cotransporter.  $-J(\text{B}^- \text{min}^{-1})$  and  $J(\text{B}^- \text{min}^{-1})$  were calculated from the  $\Delta\text{pH}/\Delta t$  obtained by linear regression analysis of the  $\text{pH}_i$  measurements made over the first 30 or 60 s, respectively ( $n = 44\text{--}76$  ROIs/3–5 ducts/3 mice/groups). For the regeneration from the alkaline load  $P = 0.2144$  (acute glucose) and 0.5524 (chronic glucose) vs. Control, using the Kruskal–Wallis test. For regeneration from the acidic load, ns:  $P = 0.9702$  vs. Control,  $*P = 0.0175$  vs. Control and  $**P < 0.0001$  vs. Acute glucose, using the Kruskal–Wallis test. B, activity of the  $\text{Cl}^-/\text{HCO}_3^-$  exchanger was measured using the  $\text{Cl}^-$  withdrawal technique. Bar charts showing the rate of regeneration from alkalosis after re-administration of extracellular  $\text{Cl}^-$  (Ba) and the maximal  $\text{pH}_i$  change (Bb).  $-J(\text{B}^- \text{min}^{-1})$  was calculated from the  $\Delta\text{pH}/\Delta t$  obtained by linear regression analysis of the  $\text{pH}_i$  measurements made over the first 60 s ( $n = 44\text{--}60$  ROIs/3–4 ducts/3 mice/groups). For the regeneration from the alkaline load,  $P < 0.9999$ . For  $\text{pH}_i$  change,  $P = 0.7677$  (acute glucose) and 0.2583 (chronic glucose) vs. Control, using the Kruskal–Wallis test.



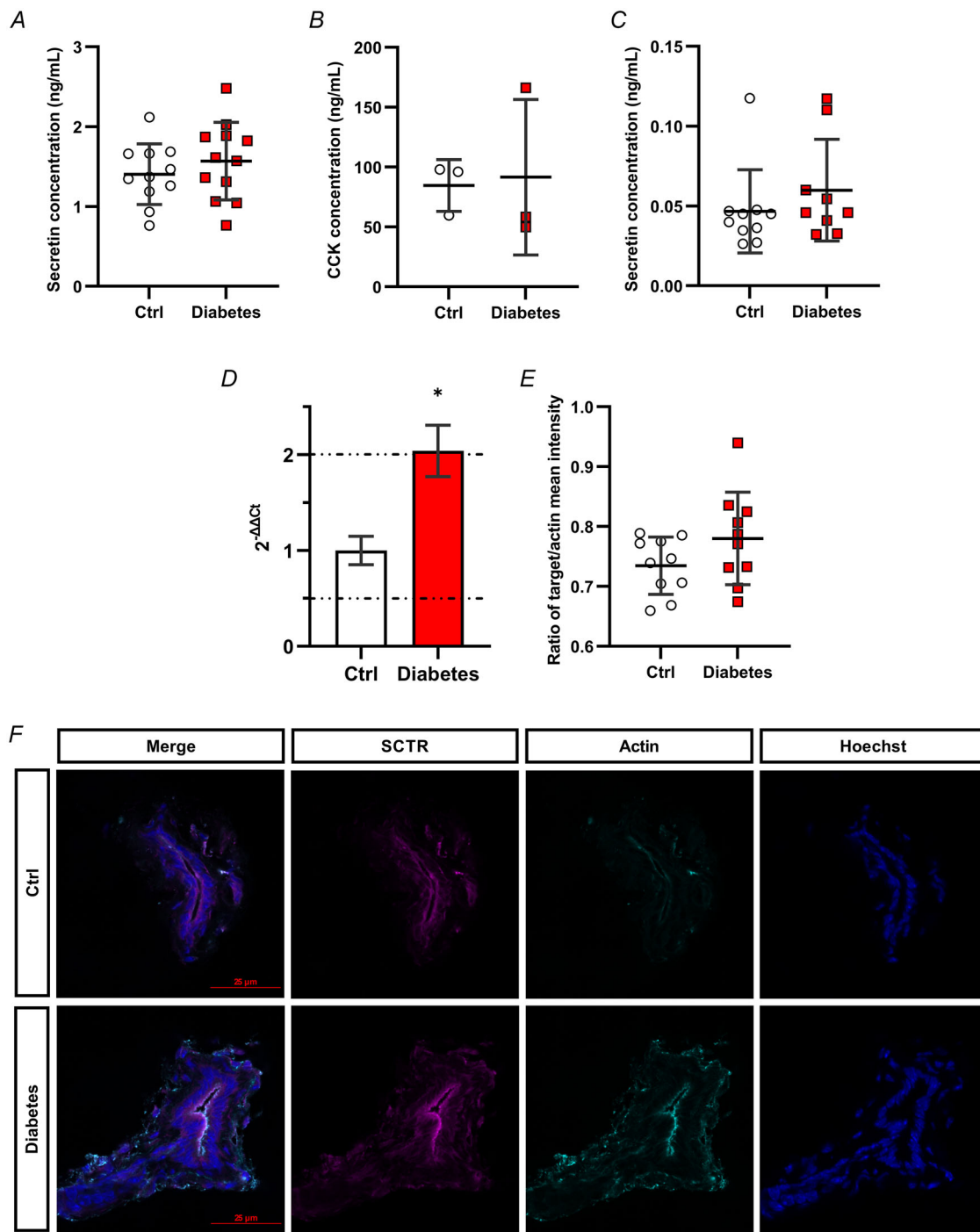


**Figure 8. Effect of diabetes on secretin and cholecystokinin levels and the expression of SCTR**

Plasma and pancreas samples were obtained from control and diabetic mice and the serum levels of secretin (A) and cholecystokinin (B) and the levels of secretin in the pancreas homogenate (C) were measured by ELISA. Data are shown as the mean  $\pm$  SD ( $n = 3$ – $12$  mice/groups).  $P = 0.3803$  for serum secretin,  $P = 0.8689$  for serum cholecystokinin and  $P = 0.3337$  for tissue homogenate secretin, using a two-sample  $t$  test. Intra-interlobular pancreatic ducts were isolated from control and diabetic mice and the mRNA (D) and protein (E and F) expression of SCTR were measured by RT-PCR and immunostaining, respectively. SCTR mRNA expression values  $\leq 0.5$  were considered to be downregulated, whereas values  $\geq 2$  were considered to be upregulated. Data are shown as the mean  $\pm$  SD. For secretin protein expression,  $n = 10$  ROIs/4 ducts/3 mice/groups.  $P = 0.1311$  using a two-sample  $t$  test.

the activity of CFTR using a  $\text{Cl}^-$  sensitive fluorescent dye along with the specific CFTR activator, forskolin. We detected increased CFTR activity in diabetic ducts, which presumably contributes to an increased rate of  $\text{HCO}_3^-$  secretion. The  $\text{NH}_4\text{Cl}$  pre-pulse technique also enables the investigation of alkalizing transporters by measuring the rate of regeneration from acidosis. Similar to alkali recovery, we observed a significant increase in acid recovery, indicating that the activity of alkalizing transporters was also increased as a result of diabetes. In ductal cells, the major alkalizing transporters are NHE and NBC. NHE is an electroneutral transporter that mediates the exchange of intracellular  $\text{H}^+$  to extracellular  $\text{Na}^+$ , whereas NBC is an electrogenic co-transporter, through which  $\text{Na}^+$  and  $\text{HCO}_3^-$  enter the cell with isotype-dependent stoichiometry. Both transporters have an important role in ductal  $\text{HCO}_3^-$  secretion because NBC promotes  $\text{HCO}_3^-$  accumulation, whereas NHE removes  $\text{H}^+$ , a by-product of  $\text{HCO}_3^-$  from the cell (Lee et al., 2012). Consequently, if the activity of the anion exchanger increases, NHE and NBC activity also increases, as confirmed by our experiments.

Next, we identified the mechanism which is responsible for increased transporter activity. As a first step, we measured the expression of the major acid-base transporters. We found that both the mRNA and protein expression of CFTR was significantly increased in diabetic ducts, which may explain the increased activity of CFTR in diabetes. In addition, overexpression of other acid-base transporters, which are involved in the  $\text{HCO}_3^-$  secretion, was also observed as a result of diabetes. ANO-1 or TMEM16A is a  $\text{Ca}^{2+}$ -activated  $\text{Cl}^-$  channel that exhibits multiple cellular functions in the body, including the regulation of epithelial secretion (Dulin, 2020). The presence of ANO-1 has been confirmed in salivary and pancreatic acini (Huang et al., 2009; Romanenko et al., 2010), but not in ductal cells. Although, the presence of a  $\text{Ca}^{2+}$ -activated  $\text{Cl}^-$  channel was observed in pancreatic ductal cells (Grey et al., 1989; Grey et al., 1994), the molecular identity of this channel has not yet been determined. The present study is the first to demonstrate the presence of ANO-1 on the luminal membrane of ductal cells and we found that diabetes increases the expression of this  $\text{Cl}^-$  channel. The antibody we used is directed against the third extracellular loop of mouse ANO-1 and has been shown to be highly specific against the protein (Dauner et al., 2012). ANO-1 has been intensively studied subsequent to its discovery. It has been shown that the channel can be activated by divalent cations, especially by  $\text{Ca}^{2+}$  (Ni et al., 2014). It is conceivable that the increase in intracellular  $\text{Ca}^{2+}$  level leads to the activation of the channel also in pancreatic ductal cells, as shown in acinar cells and salivary ducts (Lee et al., 2012). However, other pathways may also be involved because, in addition to  $\text{Ca}^{2+}$ , several other

mechanisms have been described to activate the channel, such as release of extracellular ATP, decrease in intracellular pH or heat stress (Dulin, 2020).

We hypothesize that, in addition to CFTR, ANO-1 also functions in close co-ordination with the anion exchanger or acts as an alternative  $\text{HCO}_3^-$  pathway, as shown in acinar cells (Han et al., 2016). Increased expression of this channel may also contribute to increased  $\text{HCO}_3^-$  secretion in diabetes. Nevertheless, further functional studies are needed to clarify the role of ductal ANO-1 in pancreatic fluid secretion. In addition to ANO-1, the expression of AQP-1 was also increased in diabetes. AQP-1 is a constitutively expressed water channel and its presence on the plasma membrane of centroacinar cells and interlobular ducts has been demonstrated (Burghardt et al., 2003; Venglovecz et al., 2018). AQP-1 regulates transcellular water movement and, as the major water channel on ductal cells, it is responsible for the secretion of most of the fluid into the pancreatic juice (Lee et al., 2012). Overexpression of AQP-1 in diabetes is probably a compensatory mechanism for increased anion secretion because transcellular ion movements are accompanied by water transport to compensate for altered osmotic conditions. Therefore, increased AQP-1 expression may explain increased fluid secretion in diabetes. We also examined other AQP isoforms present in the pancreas (AQP-5 and -8) (Burghardt et al., 2003); however, we found no changes in their expression compared with the control. Among the NHEs, increased NHE-1 expression was also observed in diabetic ducts. Nine members of the NHE family are known, of which NHE-1 is expressed in almost every cell and it is also present on the basolateral membrane of pancreatic ducts (Lee et al., 2012). By contrast to NHE-1, we did not find alterations in the expression of NBC, indicating that NHE, rather than NBC, is responsible for the increased rate of acid regeneration in diabetes. Among the Slc26 anion exchangers, Slc26a3 and Slc26a6 isoforms occur in pancreatic ducts and play an important role in ductal  $\text{HCO}_3^-$  secretion (Lee et al., 2012). Although our functional studies revealed that  $\text{Cl}^-/\text{HCO}_3^-$  exchange activity is increased in diabetes, we found no difference in expression compared to the control. These results indicate that the increased activity of CFTR and/or ANO-1 and NHE-1 stimulates  $\text{Cl}^-/\text{HCO}_3^-$  exchange. The primary role of CFTR on stimulating the effects of diabetes is also supported by the results obtained from CFTR KO ducts and mice. In the absence of CFTR, both fluid and  $\text{HCO}_3^-$  secretion was significantly decreased compared to the control. In CFTR KO mice in which diabetes was induced, although there was a small increase in both parameters compared to the control, non-diabetic KO mice, it was not significant. This indicates that the presence of functionally active CFTR is essential for the stimulatory effect on diabetes.

We next examined the mechanism that causes the increased activity/expression of transporters during diabetes. T1DM is associated with hyperglycaemia; therefore, we tested the effect of acute and chronic glucose treatment on transporter activity. The concentration of glucose was selected based on a previous report (Futakuchi et al., 2009). Using the alkali load and  $\text{Cl}^-$  withdrawal techniques, we found that neither acute, nor chronic glucose treatment affected anion exchange activity. By contrast, chronic glucose treatment increased the rate of regeneration from acidosis, which suggests that hyperglycaemia, which occurs during diabetes, directly increases the activity of NHE and/or NBC. Previous studies showed that high extracellular glucose increases NHE-1 activity in distal nephron cells, vascular myocytes and lymphoblasts of diabetic nephropathy patients (da Costa-Pessoa et al., 2014; Davies et al., 1995; Siczkowski & Ng, 1996). These studies suggest that glucose-induced NHE-1 activity depends on protein kinase C or the Mek/Erk1/2/p90(RSK) and p38MAPK pathways, depending on the cell type. In the present study, we did not identify the mechanism by which high extracellular glucose stimulates NHE-1, although the results suggest that the stimulatory effect of diabetes on  $\text{HCO}_3^-$  secretion may include increased NHE-1 activity. In addition to hyperglycaemia, we also examined hormonal effects on secretion. The rate of  $\text{HCO}_3^-$  secretion is primarily influenced by the gastrointestinal hormone secretin, which is secreted by S cells in the duodenum (DiGregorio & Sharma, 2023). The secretion of secretin is induced at low duodenal pH, which is formed under the influence of gastric acid during a meal. The primary function of secretin is to neutralize pH in the duodenum, thus creating optimal conditions for the function of digestive enzymes (DiGregorio & Sharma, 2023). To increase duodenal pH, secretin stimulates ductal  $\text{HCO}_3^-$  through the activation of basolaterally localized secretin receptors (Ishihara et al., 1991). Activation of the secretin receptors increases intracellular cAMP levels, which increases the opening time of the CFTR channel, through phosphorylation by protein kinase A (Afroze et al., 2013). Following CFTR activation, outflow of  $\text{Cl}^-$  increases into the extracellular space. To compensate for the increased  $\text{Cl}^-$  outflow, the activity of the  $\text{Cl}^-/\text{HCO}_3^-$  exchanger increases by several fold, which results in  $\text{HCO}_3^-$  secretion. In the present study, we have demonstrated for the first time that mRNA expression of secretin receptors is significantly increased in response to diabetes. An increase was also observed at the protein level, although this was not significant. We speculate that the effect of secretin increases on ductal cells to some extent in diabetes, although further studies are needed to confirm this hypothesis.

In conclusion, our results demonstrate that the stimulatory effect of diabetes on ductal  $\text{HCO}_3^-$  secretion

is a complex process, with several factors being involved. The  $\text{Cl}^-/\text{HCO}_3^-$  exchanger activity is enhanced by the overexpression of ductal acid-base transporters, particularly CFTR and NHE-1. In addition, high extracellular glucose stimulates alkalizing transporters, such as NHE-1, which may also contribute to increased secretion. The role of the increased secretion, and also whether it is a temporary or permanent condition, is not known. It has long been known that exocrine secretion is partly under endocrine control (Camello et al., 1994; Chayvialle & Vagne, 1981). Among the endocrine hormones, insulin increases ductal fluid secretion, whereas glucagon, somatostatin and pancreatic polypeptide inhibit it (Bertelli & Bendayan, 2005). By contrast, opinions differ as to how diabetes affects ductal function. The most accepted view is that exocrine functions are mostly impaired by long-standing diabetes. One explanation for the reduced ductal secretion could be that the stimulatory effect of insulin decreases on the ductal cells. On the other hand, the present study showed that ductal secretion increases as a result of diabetes, at least in the initial stage. A recent study reported that high concentration of  $\text{HCO}_3^-$  promotes glucose-induced insulin secretion by enhancing  $\text{Ca}^{2+}$  influx (Zhang et al., 2022). Our study indicates that ductal  $\text{HCO}_3^-$  secretion serves as a protective mechanism and therefore represents a potential therapeutic target for the prevention or treatment of diabetes. Although this hypothesis is promising, further studies are needed in this area.

## References

- Afroze, S., Meng, F., Jensen, K., McDaniel, K., Rahal, K., Onori, P., Gaudio, E., Alpini, G., & Glaser, S. S. (2013). The physiological roles of secretin and its receptor. *Annals of Translational Medicine*, *1*, 29.
- Anello, M., Lupi, R., Spampinato, D., Piro, S., Masini, M., Boggi, U., Del Prato, S., Rabuazzo, A. M., Purrello, F., & Marchetti, P. (2005). Functional and morphological alterations of mitochondria in pancreatic beta cells from type 2 diabetic patients. *Diabetologia*, *48*(2), 282–289.
- Argent, B. E., Arkle, S., Cullen, M. J., & Green, R. (1986). Morphological, biochemical and secretory studies on rat pancreatic ducts maintained in tissue culture. *Quarterly Journal of Experimental Physiology*, *71*(4), 633–648.
- Behrendorff, N., Floetenmeyer, M., Schwiening, C., & Thorn, P. (2010). Protons released during pancreatic acinar cell secretion acidify the lumen and contribute to pancreatitis in mice. *Gastroenterology*, *139*(5), 1711–1720. e5, 1720 e1711-1715.
- Bertelli, E., & Bendayan, M. (2005). Association between endocrine pancreas and ductal system. More than an epiphenomenon of endocrine differentiation and development? *Journal of Histochemistry and Cytochemistry*, *53*(9), 1071–1086.

- Burghardt, B. (2003). Distribution of aquaporin water channels AQP1 and AQP5 in the ductal system of the human pancreas. *Gut*, **52**(7), 1008–1016.
- Camello, P. J., Wisdom, D. M., Singh, J., & Salido, G. M. (1994). Hormonal control of exocrine pancreatic secretion in the isolated intact rat pancreas. *Revista Espanola De Fisiologia*, **50**, 35–40.
- Chayvialle, J. A., & Vagne, M. (1981). [Hormonal control of pancreatic exocrine secretion (author's transl)]. *Gastro-entérologie Clinique Et Biologique*, **5**, 212–221.
- Creutzfeldt, W., Gleichmann, D., Otto, J., Stockmann, F., Maisonneuve, P., & Lankisch, P. G. (2005). Follow-up of exocrine pancreatic function in type-1 diabetes mellitus. *Digestion*, **72**, 71–75.
- Da Costa-Pessoa, J. M., Damasceno, R. S., Machado, U. F., Beloto-Silva, O., & Oliveira-Souza, M. (2014). High glucose concentration stimulates NHE-1 activity in distal nephron cells: The role of the Mek/Erk1/2/p90RSK and p38MAPK signaling pathways. *Cellular Physiology and Biochemistry*, **33**(2), 333–343.
- Dauner, K., Lißmann, J., Jeridi, S., Frings, S., & Möhrlen, F. (2012). Expression patterns of anoctamin 1 and anoctamin 2 chloride channels in the mammalian nose. *Cell and Tissue Research*, **347**(2), 327–341.
- Davies, J. E., Siczkowski, M., Sweeney, F. P., Quinn, P. A., Krolewski, B., Krolewski, A. S., & Ng, L. L. (1995). Glucose-induced changes in turnover of Na<sup>+</sup>/H<sup>+</sup> exchanger of immortalized lymphoblasts from type I diabetic patients with nephropathy. *Diabetes*, **44**(4), 382–388.
- De Boer, P., Pirozzi, N. M., Wolters, A. H. G., Kuipers, J., Kusmartseva, I., Atkinson, M. A., Campbell-Thompson, M., & Giepmans, B. N. G. (2020). Large-scale electron microscopy database for human type 1 diabetes. *Nature Communications*, **11**(1), 2475.
- DiGregorio, N., & Sharma, S. (2023). Physiology, Secretin. In *StatPearls*. Treasure Island (FL) ineligible companies. Disclosure: Sandeep Sharma declares no relevant financial relationships with ineligible companies.
- Dulin, N. O. (2020). Calcium-activated chloride channel ANO1/TMEM16A: Regulation of expression and signaling. *Frontiers in Physiology*, **11**, 590262.
- Fernández-Salazar, M. P., Pascua, P., Calvo, J. J., López, M. A., Case, R. M., Steward, M. C., & San Román, J. I. (2004). Basolateral anion transport mechanisms underlying fluid secretion by mouse, rat and guinea-pig pancreatic ducts. *The Journal of Physiology*, **556**(2), 415–428.
- Futakuchi, S., Ishiguro, H., Naruse, S., Ko, S. B. H., Fujiki, K., Yamamoto, A., Nakakuki, M., Song, Y., Steward, M. C., Kondo, T., & Goto, H. (2009). High glucose inhibits HCO<sub>3</sub><sup>-</sup> and fluid secretion in rat pancreatic ducts. *Pflugers Archiv: European Journal of Physiology*, **459**(1), 215–226.
- Gál, E., Dolenšek, J., Stožer, A.ž, Czaková, L., Ébert, A., & Venglovecz, V. (2021). Mechanisms of post-pancreatitis diabetes mellitus and cystic fibrosis-related diabetes: A review of preclinical studies. *Frontiers in Endocrinology (Lausanne)*, **12**, 715043.
- Gray, M. A., Harris, A., Coleman, L., Greenwell, J. R., & Argent, B. E. (1989). Two types of chloride channel on duct cells cultured from human fetal pancreas. *American Journal of Physiology*, **257**(2), C240–C251.
- Gray, M. A., Winpenny, J. P., Porteous, D. J., Dorin, J. R., & Argent, B. E. (1994). CFTR and calcium-activated chloride currents in pancreatic duct cells of a transgenic CF mouse. *American Journal of Physiology*, **266**(1), C213–C221.
- Han, Y., Shewan, A. M., & Thorn, P. (2016). HCO<sub>3</sub><sup>-</sup> transport through anoctamin/transmembrane protein ANO1/TMEM16A in pancreatic acinar cells regulates luminal pH. *Journal of Biological Chemistry*, **291**(39), 20345–20352.
- Hardt, P. D., & Ewald, N. (2011). Exocrine pancreatic insufficiency in diabetes mellitus: A complication of diabetic neuropathy or a different type of diabetes? *Experimental Diabetes Research*, **2011**, 1.
- Hardt, P. D., Hauenschild, A., Nalop, J., Marzeion, A. M., Jaeger, C., Teichmann, J., Bretzel, R. G., Hollenhorst, M., & Kloer, H. U. (2003). High prevalence of exocrine pancreatic insufficiency in diabetes mellitus. A multicenter study screening fecal elastase 1 concentrations in 1,021 diabetic patients. *Pancreatology*, **3**(5), 395–402.
- Hayden, M. R., Karuparthi, P. R., Habibi, J., Lastra, G., Patel, K., Wasekar, C., Manrique, C. M., Ozerdem, U., Stas, S., & Sowers, J. R. (2008). Ultrastructure of islet microcirculation, pericytes and the islet exocrine interface in the HIP rat model of diabetes. *Experimental Biology and Medicine (Maywood, N.J.)*, **233**(9), 1109–1123.
- Hegyí, P., Gray, M. A., & Argent, B. E. (2003). Substance P inhibits bicarbonate secretion from guinea pig pancreatic ducts by modulating an anion exchanger. *American Journal of Physiology-Cell Physiology*, **285**(2), C268–C276.
- Hegyí, P., Maléth, J., Venglovecz, V., & Rakonczay, Z. (2011). Pancreatic ductal bicarbonate secretion: Challenge of the acinar Acid load. *Frontiers in Physiology*, **2**, 36.
- Hegyí, P., Pandol, S., Venglovecz, V., & Rakonczay, Z. (2011). The acinar-ductal tango in the pathogenesis of acute pancreatitis. *Gut*, **60**(4), 544–552.
- Hegyí, P. T., Rakonczay, Z. N., Gray, M. A., & Argent, B. E. (2004). Measurement of intracellular pH in pancreatic duct cells: A new method for calibrating the fluorescence data. *Pancreas*, **28**(4), 427–434.
- Hegyí, P., Rakonczay, Z., Tiszlavicz, L., Varró, A., Tóth, A., Rácz, G., Varga, G., Gray, M. A., & Argent, B. E. (2005). Protein kinase C mediates the inhibitory effect of substance P on HCO<sub>3</sub><sup>-</sup> secretion from guinea pig pancreatic ducts. *American Journal of Physiology-Cell Physiology*, **288**(5), C1030–C1041.
- Huang, F., Rock, J. R., Harfe, B. D., Cheng, T., Huang, X., Jan, Y. N., & Jan, L. Y. (2009). Studies on expression and function of the TMEM16A calcium-activated chloride channel. *The Proceedings of the National Academy of Sciences*, **106**(50), 21413–21418.
- Ishihara, T., Nakamura, S., Kaziro, Y., Takahashi, T., Takahashi, K., & Nagata, S. (1991). Molecular cloning and expression of a cDNA encoding the secretin receptor. *Embo Journal*, **10**(7), 1635–1641.

- Laczko, D., Rosztoczy, A., Birkas, K., Katona, M., Rakonczay, Z., Tiszlavicz, L., Roka, R., Wittmann, T., Hegyi, P., & Venglovecz, V. (2016). Role of ion transporters in the bile acid-induced esophageal injury. *American Journal of Physiology-Gastrointestinal and Liver Physiology*, **311**(1), G16–G31.
- Lee, M. G., Ohana, E., Park, H. W., Yang, D., & Muallem, S. (2012). Molecular mechanism of pancreatic and salivary gland fluid and HCO<sub>3</sub> secretion. *Physiological Reviews*, **92**(1), 39–74.
- Mossner, J., Logsdon, C. D., Goldfine, I. D., & Williams, J. A. (1984). Regulation of pancreatic acinar cell insulin receptors by insulin. *American Journal of Physiology*, **247**, G155–G160.
- Mossner, J., Logsdon, C. D., Williams, J. A., & Goldfine, I. D. (1985). Insulin, via its own receptor, regulates growth and amylase synthesis in pancreatic acinar AR42J cells. *Diabetes*, **34**(9), 891–897.
- Ni, Y.u-Li, Kuan, A.i-S., & Chen, T-Y. U. (2014). Activation and inhibition of TMEM16A calcium-activated chloride channels. *PLoS ONE*, **9**(1), e86734.
- Okabayashi, Y., Otsuki, M., Ohki, A., Nakamura, T., Tani, S., & Baba, S. (1988). Secretin-induced exocrine secretion in perfused pancreas isolated from diabetic rats. *Diabetes*, **37**(9), 1173–1180.
- Okabayashi, Y., Otsuki, M., Ohki, A., Suehiro, I., & Baba, S. (1988). Effect of diabetes mellitus on pancreatic exocrine secretion from isolated perfused pancreas in rats. *Digestive Diseases and Sciences*, **33**(6), 711–717.
- Park, H. W., Nam, J. H., Kim, J. Y., Namkung, W., Yoon, J. S., Lee, J.-S., Kim, K. S., Venglovecz, V., Gray, M. A., Kim, K. H., & Lee, M. G. (2010). Dynamic regulation of CFTR bicarbonate permeability by [Cl<sup>-</sup>]<sub>i</sub> and its role in pancreatic bicarbonate secretion. *Gastroenterology*, **139**(2), 620–631.
- Pascua, P., García, M., Fernández-Salazar, M. P., Hernández-Lorenzo, M. P., Calvo, J. J., Colledge, W. H., Case, R. M., Steward, M. C., & San Román, J. I. (2009). Ducts isolated from the pancreas of CFTR-null mice secrete fluid. *Pflugers Archiv: European Journal of Physiology*, **459**(1), 203–214.
- Patel, R., Singh, J., Yago, M. D., Vilchez, J. R., Martínez-Victoria, E., & Mañas, M. (2004). Effect of insulin on exocrine pancreatic secretion in healthy and diabetic anaesthetised rats. *Molecular and Cellular Biochemistry*, **261**(1), 105–110.
- Perides, G., Van Acker, G. J.d, Laukkarinen, J. M., & Steer, M. L. (2010). Experimental acute biliary pancreatitis induced by retrograde infusion of bile acids into the mouse pancreatic duct. *Nature Protocols*, **5**(2), 335–341.
- Piciocchi, M., Capurso, G., Archibugi, L., Delle Fave, M. M., Capasso, M., & Delle Fave, G. (2015). Exocrine pancreatic insufficiency in diabetic patients: Prevalence, mechanisms, and treatment. *International Journal of Endocrinology*, **2015**, 1.
- Radlinger, B., Ramoser, G., & Kaser, S. (2020). Exocrine Pancreatic Insufficiency in Type 1 and Type 2 Diabetes. *Current Diabetes Reports*, **20**(6), 18.
- Rodriguez-Calvo, T., Ekwall, O., Amirian, N., Zapardiel-Gonzalo, J., & Von Herrath, M. G. (2014). Increased immune cell infiltration of the exocrine pancreas: A possible contribution to the pathogenesis of type 1 diabetes. *Diabetes*, **63**(11), 3880–3890.
- Romanenko, V. G., Catalán, M. A., Brown, D. A., Putzier, I., Hartzell, H. C., Marmorstein, A. D., Gonzalez-Begne, M., Rock, J. R., Harfe, B. D., & Melvin, J. E. (2010). Tmem16A encodes the Ca<sup>2+</sup>-activated Cl<sup>-</sup> channel in mouse submandibular salivary gland acinar cells. *Journal of Biological Chemistry*, **285**(17), 12990–13001.
- Shcheynikov, N., Wang, Y., Park, M., Ko, S. B. H., Dorwart, M., Naruse, S., Thomas, P. J., & Muallem, S. (2006). Coupling modes and stoichiometry of Cl<sup>-</sup>/HCO<sub>3</sub><sup>-</sup> exchange by slc26a3 and slc26a6. *Journal of General Physiology*, **127**(5), 511–524.
- Siczkowski, M., & Ng, L. L. (1996). Glucose-induced changes in activity and phosphorylation of the Na<sup>+</sup>/H<sup>+</sup> exchanger, NHE-1, in vascular myocytes from Wistar-Kyoto and spontaneously hypertensive rats. *Metabolism*, **45**(1), 114–119.
- Thomas, J. A., Buchsbaum, R. N., Zimniak, A., & Racker, E. (1979). Intracellular pH measurements in Ehrlich ascites tumor cells utilizing spectroscopic probes generated in situ. *Biochemistry*, **18**(11), 2210–2218.
- Venglovecz, V., Pallagi, P., Kemeny, L. V., Balazs, A., Balla, Z., Becskhazi, E., Gal, E., Toth, E., Zvara, A., Puskas, L. G., Borka, K., Sandler, M., Lerch, M. M., Mayerle, J., Kuhn, J. P., Rakonczay, Z., Jr., & Hegyi, P. (2018). The importance of aquaporin 1 in pancreatitis and its relation to the CFTR Cl<sup>-</sup> channel. *Frontiers in Physiology*, **9**, 854.
- Wang, Y., Soyombo, A. A., Shcheynikov, N., Zeng, W., Dorwart, M., Marino, C. R., Thomas, P. J., & Muallem, S. (2006). Slc26a6 regulates CFTR activity in vivo to determine pancreatic duct HCO<sub>3</sub><sup>-</sup> secretion: Relevance to cystic fibrosis. *Embo Journal*, **25**(21), 5049–5057.
- Weintraub, W. H., & Machen, T. E. (1989). pH regulation in hepatoma cells: Roles for Na-H exchange, Cl-HCO<sub>3</sub> exchange, and Na-HCO<sub>3</sub> cotransport. *American Journal of Physiology*, **257**, G317–G327.
- Zhang, Y.-C., Xiong, F.-R., Wang, Y.-Y., Shen, H., Zhao, R.u-X., Li, S., Lu, J., & Yang, J.-K. (2022). High bicarbonate concentration increases glucose-induced insulin secretion in pancreatic beta-cells. *Biochemical and Biophysical Research Communications*, **589**, 165–172.
- Zsóri, G., Illés, D., Terzin, V., Ivány, E., & Czako, L. (2018). Exocrine pancreatic insufficiency in type 1 and type 2 diabetes mellitus: Do we need to treat it? A systematic review. *Pancreatology*, **18**(5), 559–565.

## Additional information

### Data availability statement

All data ( $n \leq 30$ ) supporting the findings of this study the present available within the paper. All other data ( $> 30$ ) are available at online (<https://figshare.com/account/items/24899709>) or will be made available from the corresponding author upon reasonable request.

### Competing interests

The authors declare that they have no competing interests.

### Author contributions

A.É. performed all of the experiments and analysed the data. E.G. performed the RT-PCR. E.T. was involved in the pancreatic fluid and  $\text{HCO}_3^-$  measurements. T.S. performed electron microscopy. P.H. was involved in data interpretation and edited the manuscript. V.V. supervised the project and drafted the manuscript. All authors approved the final version of the manuscript submitted for publication.

### Funding

CF-Trust CFRD-SRC: Attila Ébert, Emese Tóth, Péter Hegyi, Viktoria Venglovecz, SRC 007; National Research, Development and Innovation Office: Attila Ébert, Eleonóra Gál, Viktoria Venglovecz, SNN134497

### Acknowledgements

We are grateful for support for this study provided by the CF-Trust CFRD-SRC Grant (No.: SRC 007) and the National Research, Development and Innovation Office (SNN134497) and New National Excellence Program Of The Ministry Of Human Capacities (UNKP-18-4 to VV).

### Keywords

CFTR, diabetes, endocrine-exocrine interaction, fluid and  $\text{HCO}_3^-$  secretion, pancreatic ductal cells, secretin

### Supporting information

Additional supporting information can be found online in the Supporting Information section at the end of the HTML view of the article. Supporting information files available:

### Peer Review History